Structural Changes in the Actin–Myosin Cross-Bridges Associated with Force Generation Induced by Temperature Jump in Permeabilized Frog Muscle Fibers

Andrey K. Tsaturyan*, Sergey Y. Bershitsky#, Ronald Burns, and Michael A. Ferenczi

*Institute of Mechanics, Moscow University, Mitchurinsky prosp. 1, Moscow 119899, Russia, #Institute of Physiology, Ural Branch, Russian Academy of Sciences, Yekaterinburg 620102 Box 105, Russia, and National Institute for Medical Research, The Ridgeway, Mill Hill, London NW7 1AA, United Kingdom

ABSTRACT Structural changes induced by Joule temperature jumps (T-jumps) in frog muscle fibers were monitored using time-resolved x-ray diffraction. Experiments made use of single, permeabilized fibers that were fully activated after slight cross-linking with 1-ethyl-3-[3-dimethylamino)propyl]carbodiimide to preserve their structural order. After T-jumps from 5–6 to ~17°C and then on to ~30°C, tension increased by a factor of 1.51 and 1.84, respectively, whereas fiber stiffness did not change with temperature. The tension rise was accompanied by a decrease in the intensity of the (1, 0) equatorial x-ray reflection by 15 and 26% (at ~17 and ~30°C) and by an increase in the intensity of the M3 myosin reflection by 20% and 41%, respectively. The intensity of the (1, 1) equatorial reflection increased slightly. The peak of the intensity on the 6th actin layer line shifted toward the meridian with temperature. The intensity of the 1st actin layer line increased from 12% (of its rigor value) at 5–6°C to 36% at ~30°C, so that the fraction of the cross-bridges labeling the actin helix estimated from this intensity increased proportionally to tension from ~35% at 5–6°C to ~60% at ~30°C. This suggests that force is generated during a transition of nonstereo-specifically attached myosin cross-bridges to a stereo-specific binding state.

INTRODUCTION

Muscle force results from a tilting movement of myosin cross-bridges attached to actin filaments in muscle fibers (Reedy et al., 1965; Huxley, 1969). However, the nature of the conformational change in the actin–myosin complex that induces force generation in muscle is uncertain. Because the cross-bridges generate force asynchronously, external perturbations that force them to act simultaneously make it easier to monitor macroscopic and microscopic mechanical and structural changes in a large fraction of the cross-bridges. Since the classical papers of Huxley and Simmons (1971) and Ford et al., (1977), fast length changes have been used by a number of investigators to synchronize cross-bridge processes in contracting muscle. Following quick releases or stretches during isometric contraction of an intact frog muscle, a transitional decrease in the intensity of the meridional x-ray reflection on the 3rd myosin layer line (M3) was observed (Huxley et al., 1981, 1983). Because the M3 reflection arises from an axial repeat of myosin cross-bridges on the thick filaments (Huxley and Brown, 1967), these changes suggest that a large fraction of the cross-bridges tilts in response to the perturbation. Similar experiments were done with single intact muscle fibers of the frog with 0.2 ms time resolution and with control of the sarcomere length (Irving et al., 1992; Lombardi et al., 1995; Piazzesi et al., 1995). It was found that the decrease in the intensity of the M3 reflection following a quick 0.5% decrease in muscle length does not occur during the release itself, but follows the fast partial tension recovery that occurs after the end of the applied length change (Irving et al., 1992). Small changes in orientation of fluorescent probes attached to the light chains on the necks of myosin cross-bridges following a length step were also observed (Irving et al., 1995; Hopkins et al., 1998). Thus, there is evidence for a tilt of a fraction of myosin cross-bridges attached to actin after a length perturbation. This, however, does not necessarily mean that the process that induces the fast partial tension recovery and the tilt of the cross-bridges following a length change is responsible for the force-generating transitions in the cross-bridges that drive muscle contraction (Brenner, et al., 1995). A hypothesis that these processes are equivalent was put forward by Huxley and Simmons (1971), however, later, Huxley (1981) pointed out that some independent evidence is needed to validate this idea.

An alternative way to synchronize force-generating transitions in myosin cross-bridges without significant movement of the thin and thick filaments is to rapidly increase the fiber temperature (Goldman et al., 1987; Bershitsky and Tsaturyan, 1988; Tsaturyan and Bershitsky, 1988; Davis and Harrington, 1993; Davis and Rodgers, 1995; Ranatunga, 1996). A Joule temperature jump (T-jump, induced by passing a current through the muscle fiber) induces a substantial increase in isometric tension in a fully activated permeabilized muscle fiber (Bershitsky and Tsaturyan, 1989, 1992). Structural changes accompanying the tension rise were monitored using time-resolved low-angle x-ray diffraction on beam line 16.1 of the Synchrotron Radiation Source in Daresbury Laboratory (Cheshire, U.K.). Slight

Received for publication 2 June 1998 and in final form 19 March 1999.

Address reprint requests to Dr. M. A. Ferenczi, National Institute for Medical Research, The Ridgeway, Mill Hill, London NW7 1AA, U.K. Tel.: +44–181-9593666 ext. 2077; Fax: +44–181-9064419; E-mail: m-ferenc@nimr.mrc.ac.uk.

0006-3495/99/07/354/19 $2.00

cross-linking of the contractile proteins with 1-ethyl-3-[3-dimethylamino)propyl]carbodiimide (EDC) was used to reduce deterioration of sarcomere structure during long-term activation of permeabilized frog muscle fibers (Bershitsky et al., 1996). Results of the x-ray diffraction T-jump experiments were published in brief (Bershitsky et al., 1997). Here, we present another set of experiments in which double T-jumps from ~5 to ~17°C and again to ~30°C were applied to muscle fibers to cover a wider range of temperature and isometric force and to collect x-ray diffraction patterns with better resolution.

METHODS

Muscle fiber preparation and apparatus

The muscle fiber preparation and details of the apparatus were described by Bershitsky et al. (1996). Briefly, single fibers (segments 3–3.5 mm long, 120–140 μm in diameter) from the semitendinosus muscle of *Rana temporaria* were permeabilized by 15–30 min treatment in relaxing solution (see below) containing 0.5% Triton X-100 at 5–10°C, 15 min in relaxing solution containing 25% (v/v) glycerol for 15 min and again 15 min in solution containing 50% (v/v) glycerol, before mounting in the apparatus in glycerol-free relaxing solution. A fiber was mounted horizontally with one end glued to a force transducer and the other to a linear motor by means of a shellac/ethanol paste (Bershitsky and Tsaturyan, 1992). The piezo-electric force transducer had a resonance frequency of 12–15 kHz with a time constant of electric charge drain $\geq$10 s and noise corresponding to $<$5 μN. The linear motor had peak-to-peak noise of 50 nm, a linear displacement range of 200 μm and allowed step displacements $\pm$50 μm in 0.14 ms. The sarcomere length was monitored during the experiments by diffraction, using a 2 mW He-Ne laser. To preserve sarcomere structure from deterioration during activation, slight cross-linking with EDC was used (Bershitsky and Tsaturyan, 1995b; Bershitsky et al., 1996).

Solutions

Two rigor solutions were used, composed as follows: a) 5 mM EDTA, 100 mM 3-[N-morpholino]propanesulfonic acid (MOPS), 120 mM potassium propionate, or b) 2 mM $MgCl_2$, 5 mM EGTA, 100 mM MOPS, 110 mM potassium propionate. The prerigor solution (Bershitsky et al., 1996) contained 5–10 mM 2,3-butanedione monoxime (BDM), 0.4 mM Na_2ATP, 2 mM $MgCl_2$, 5 mM EGTA, 100 mM MOPS and 110 mM potassium propionate; 5 mM BDM was added to the rigor solution to get rigor state with well ordered sarcomeres (Higuchi et al., 1995; Bershitsky et al., 1996). When full rigor stiffness developed in a fiber at low tension, BDM was washed out. Fibers were then treated with 10 mM EDC in the presence of 2 mM $MgCl_2$, 60 mM inorganic phosphate at 15°C for 10–15 min depending on fiber diameter. Then EDC was washed out with the same phosphate buffer. The activating solution contained 100 mM MOPS, 10 mM CaEGTA, 5.5 mM Na_2ATP, 7.5 mM $MgCl_2$, 22 mM phosphocreatine (PCr) and 1.5 mg/mL chicken creatine kinase with high specific activity (Bershitsky et al., 1996). The relaxing solution had the same composition, except that CaEGTA was substituted by EGTA and the concentration of PCr was increased to 25 mM. To detach all unlinked cross-bridges from actin in EDC-treated fibers, a super-relaxing solution containing 50 mM BDM, 20 mM inorganic phosphate, 5.5 mM Na_2ATP, 7.5 mM $MgCl_2$, 5 mM EGTA, 20 mM PCr was used (Bershitsky et al., 1996). All solutions were at pH 7.1 at 20°C with an ionic strength of ~0.2 M.

T-jump

The T-jump method was described previously by Bershitsky and Tsaturyan (1992, 1995a). The fiber temperature was increased in a period lasting 0.5–0.8 ms by passing a high voltage (up to 3 kV) pulse from an AC (~30 kHz) power supply while the fiber was suspended in air in a cold (5–6°C), water-saturated atmosphere. The amplitude of the T-jump was calculated by dividing the heat energy liberated in a fiber by its thermal capacity. The thermal capacity was estimated as previously (Bershitsky and Tsaturyan, 1992, 1995a) using the fiber volume determined by microscopical measurement of its dimensions while suspended in air, a fiber density of 1.06 $kg \cdot m^{-3}$ and a specific heat capacity of 3.7 $kJ \cdot kg^{-1} \cdot K^{-1}$ (Hill, 1931). Fiber volume measurements in air were indistinguishable from measurements carried out with the fiber immersed in solution. To overcome the slow cooling of the fiber after the T-jump, a warming AC current (30 kHz) of several hundred volts amplitude was applied after the heating pulse. The amount of energy applied to the fiber in the T-jump was calculated on-line by means of an electronic device measuring AC voltage and current applied to a fiber (Bershitsky and Tsaturyan, 1995a), taking into account the capacitance in the wires connected to the fiber. The energy is the integration of the product of voltage and current during the applied pulse. It was found that the determination of fiber temperature resulting from calculations of T-jump energy carried out in the laboratory were different from calculations performed at the Daresbury Synchrotron. The difference is attributed to electronic interference in the experimental hutch at the synchrotron, which changed the estimate of wire capacitance. Careful analysis of the instrument revealed that, in the previous work (Bershitsky et al., 1997), the amplitude of the temperature change had been underestimated by 3°C. This means that the temperature jump that achieved a 1.68-fold increase in force was from 5–6°C to 20.5 $\pm$ 1.5°C and not to 16–19°C, as stated by Bershitsky et al. (1997).

Experimental procedure

At the beginning of each experiment, relaxed and rigor diffraction patterns were collected in air at 5–6°C for 1 s each while the muscle fiber was suspended in air. After partial EDC cross-linking, the diffraction pattern in rigor was collected again for 5 s. Then, the fiber was activated at 0–1°C, and this state lasted for 1–2 h of experiment without relaxation. The activating solution that contained the ATP back-up system was changed every 20 min. As a result of EDC cross-linking, the structural and mechanical properties did not change significantly during the long activation (Bershitsky et al., 1996). Time-resolved x-ray diffraction patterns were obtained during the double T-jump protocol (see below) from contracting fibers. At the end of nine of the experiments, the fiber was immersed in super-relaxing solution, and the x-ray diffraction pattern was collected in air for 10 s. At the end of five of the experiments, the fibers were put into Mg-free rigor solution, and the x-ray diffraction patterns were collected during the double T-jump protocol.

X-ray diffraction

Time-resolved 2D x-ray diffraction patterns were collected with a gas-filled electronic detector (Worgan et al., 1990) on beam line 16.1 at the Synchrotron Radiation Source at Daresbury as described by Bershitsky et al. (1996, 1997). The fiber-to-detector distance was 4.34 m. The x-ray beam was focused at the fiber in the vertical direction to maximize photon flux through the fiber, and was focused horizontally at the detector to sharpen the reflection peaks along the meridian. A 14-mm square beam stop was placed in the evacuated beam pipe as near to the detector as possible to absorb the undiffracted x-rays. The center of the electronic detector was shifted horizontally off the x-ray beam, so that 6th and 7th actin layer lines (A6 and A7) at ~$(5.9\ nm)^{-1}$ and ~$(5.1\ nm)^{-1}$, respectively, were seen on one side of the detector (see Fig. 9). The center of the lead beam-stop was horizontally off-center, 54 mm away from the edge of the beam pipe. The extent of offset was such that all four quadrants of the diffraction pattern could still be used for measurement of the main equatorial and main meridional reflections.

The patterns were corrected for response of the detector, and camera background scattering was subtracted. BSL, XOTOKO and XFIT software

obtained from CCP13 (Daresbury Laboratory, Cheshire, U.K.) was used for the analysis of the x-ray data.

Double T-jump protocol

To collect the x-ray diffraction data at three different temperatures, a double T-jump protocol was used (see Fig. 4). At the beginning of the protocol, the activated fiber was suspended in air and its temperature increased from 0–1 to 5–6°C. Two seconds later, the protocol began. To measure fiber stiffness, it was released by 0.5% of its length in 140 μs and, 10 ms later, restretched to the initial length. After 0.2 s of isometric contraction, the fast shutter was opened and the fiber was exposed to the x rays. Then, 0.2 s later, the first T-jump to 17.1 ± 0.4°C (range 14–19°C) was applied and tension increased. Because the data scattering was mainly due to differences between muscle fibers, whereas, for each fiber, the amplitude of the temperature changes and the tension transients were reproducible, the data are presented as mean ± SE, $n = 16$, where n is the number of fibers, unless otherwise stated. Approximately 50 ms after the T-jump, tension achieved a new steady-state level. The second T-jump, 0.25 s after the first T-jump, to 29.5 ± 0.8°C (range 24–33°C) was applied. Again, it took about 50 ms for tension to reach a new steady-state level. The shutter was closed 0.25 s after the second T-jump and the release–stretch cycle was repeated to measure stiffness at the higher temperature. X-ray framing during the double T-jump protocol is shown in Fig. 4 *A*. The x-ray data were stored into two 100-ms time frames at the plateau of contraction at low (5–6°C) temperature. Then, 16 frames of 1-ms duration were collected so that the beginning of the T-jump was synchronized with the beginning of the seventh 1-ms frame. The rate of framing was then decreased and eight frames of 5-ms duration were recorded. Two 50-ms frames followed by a 100-ms frame were collected at the plateau of tension following the T-jump. Identical framing schemes were used for the first and second T-jumps. The fiber was returned to the trough containing the activating solution and the protocol was repeated 1–2 min later.

The double T-jump protocol was run 417 times in 16 frog muscle fibers (8–50 runs per fiber) until isometric tension at the lower temperature decreased to 85% of its initial value. In five experiments, after 30–40 runs of the protocol in the activating solution, muscle fibers were put into EDTA rigor solution, and the double T-jump was applied 10 to 15 times.

2D diffraction patterns

To obtain high signal-to-noise ratio, the x-ray diffraction patterns in different states were summed from several muscle fibers. The active diffraction patterns were collected during the double T-jump protocol.

Individual diffraction patterns in relaxed, rigor, and super-relaxed states were normalized for the x-ray exposure of the same fiber during contraction at low temperature (0.2-s plateaus of isometric contraction at 5–6°C, see Fig. 4) and for the reading of the ion chamber, which was considered to be proportional to the brightness of the x-ray beam. The last correction was necessary because the rigor and relaxed patterns were always collected at the beginning of the experiment when the beam was usually brighter, whereas the super-relaxed patterns were collected at the end of the experiment when the beam had decayed. The patterns were then added together. This procedure provided the same contribution from each fiber for the rigor, relaxed, and active patterns, so these patterns could be compared quantitatively as if they were collected from a single fiber.

Measurement of equatorial reflections and of the main meridional reflection

The time course of the intensities of the main equatorial reflections (1, 0) and (1, 1) was followed throughout the protocols. The 2D x-ray diffraction patterns in each time frame were symmetrically averaged in four quadrants and integrated across the equator within the region of the (1, 0) and (1, 1) peaks. The integrated 1D patterns were then analyzed using XFIT software and fitted by Gaussian curves, so that the positions, widths, and intensities of the (1, 0) and (1, 1) x-ray diffraction peaks were determined for each time frame after subtraction of a polynomial background. A small reflection originating from the muscle fiber Z-lines, which appears between the (1, 0) and (1, 1) reflections, was included in the fitting procedure.

A similar procedure was adopted for measurement of the time course of changes in the main meridional reflection on M3.

RESULTS

X-ray diffraction pattern in different states of the fibers at low temperature

The x-ray diffraction patterns in different states were obtained in nine experiments to characterize the main structural features of partially EDC cross-linked muscle fibers used in T-jump experiments. The active patterns were collected during 0.2-s plateaus of isometric contraction at 5–6°C at the beginning of the double T-jump protocol. The protocol was repeated 13–50 times, and the patterns obtained from each fiber were summed so that total exposure was 45.4 s. Individual diffraction patterns in relaxed, rigor, and super-relaxed states were normalized for the x-ray exposure of the same fiber during contraction at low temperature and for the reading of the ion chamber. For the relaxed and rigor patterns, which were collected before activation, the ion chamber readings were 1.10 ± 0.07 and 1.09 ± 0.01 (mean ± SE, $n = 9$) of their average value during active contraction. For the super-relaxed patterns, recorded 1–2 h after the fiber was activated, the ion chamber reading was 0.93 ± 0.02 of that during contraction. The patterns from individual fibers were then added together.

Figure 1 shows the diffraction patterns obtained with this procedure. The myosin layer lines M1, M2, and M3 are clearly seen in the relaxed fibers, and the actin layer lines A1 and A2 are seen in rigor. We found no difference in the rigor diffraction patterns collected before and after EDC cross-linking: the spacing and the intensity of the main equatorial and meridional reflections and of the actin layer lines were the same within the accuracy of our experiments. During contraction, the intensities of the actin and myosin layer lines (except the meridional spot on M3) were greatly reduced compared to those in the rigor and relaxed states, respectively. The M3 intensity, I_{M3}, was slightly lower than in relaxed fibers and ~3-fold higher than in rigor. The intensity of the M3 reflection was significantly spread along the equator. This equatorial spread is typical for contracting muscle, and results from axial disorder of neighboring myosin filaments (Huxley et al., 1982). The broadening of the M3 reflection during contraction of EDC-treated frog muscle fibers shows that cross-linking did not prevent the disordering of filaments resulting from the active force developed by uncross-linked myosin heads.

There was also a remainder of the 1st actin/myosin layer line (LL1) at $(36–43\ \text{nm})^{-1}$ during active contraction at low temperature (Fig. 2 *A*). The intensity of this layer line was, however, much lower than that of M1 in relaxed fibers or A1 in rigor. In the super-relaxing solution, the intensity of LL1 reduced further compared to that of active contraction.

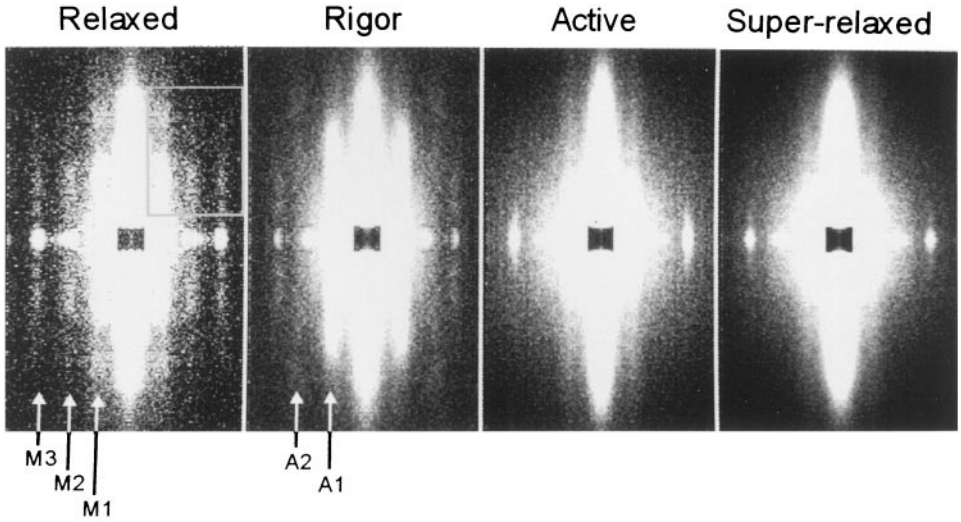

FIGURE 1 2D x-ray diffraction patterns from frog muscle fibers in different states at 5–6°C. The patterns obtained from 9 permeabilized frog muscle fibers in the relaxed state, in rigor, at the plateau of isometric contraction, and in the super-relaxing solution are shown. Higher intensity is shown as white and the equator is vertical. The dark rectangle in the middle of the patterns is the shadow of the beam stop. Individual patterns were corrected for the detector response and for the camera background scattering and symmetrically averaged in four quadrants. The patterns from different fibers were summed after correction for exposure of each fiber in each state and for the brightness of the beam as described in the Results section. The myosin M1–M3 and actin A1, A2 layer lines are labeled. The gray rectangle is the area of equatorial integration used for the intensity profiles shown in Figs. 2 *A* and 3.

This shows that the helical structure formed by the myosin heads being packed in close proximity to the myosin filament was not restored by a high concentration of BDM and P_i. The intensity of LL1 in the super-relaxing solution was small compared to background, so it was difficult to measure the intensity and the position of this layer line. Two different algorithms of decomposition of LL1 intensity into components corresponding to M1 of relaxed fibers and A1 found in rigor showed that the intensity of the M1 component was slightly less and the A1 component was about two-fold less than their values during active contraction.

As the intensity of the layer lines decreases in both activating and super-relaxing solutions, one would expect the background to increase, because the total x-ray intensity scattered by the fiber must be constant. However, we observed a decrease in the background level during active contraction and especially in the super-relaxing solution compared to the relaxed and rigor patterns. This can be explained by the fact that each diffraction pattern was corrected for the camera background scattering collected for 60 s at the end of each experiment after the fiber was removed from the set-up. This camera background pattern was scaled for exposure, but no correction for the ion chamber reading was done at this stage of the analysis. By the time the camera background pattern was recorded, the ion chamber reading was 0.90 ± 0.02 ($n = 9$) of that during active contraction. Therefore, we underestimated the camera scattering (and therefore overestimated the fiber background scattering) for the patterns obtained at the beginning of the experiments. For this reason, the background for the active, and especially for the super-relaxed pattern taken right at the end of each fiber experiment, seems to be lower than those for relaxed and rigor fibers (Fig. 2 *A*).

Figure 2 *B* shows equatorial intensity profiles for the patterns shown in Fig. 1. In the super-relaxing solution, the intensity $I_{1,1}$ of the equatorial reflection (1, 1) changed toward its relaxed value, but did not recover completely. The intensity of the (1, 0) reflection was, however, much lower than in relaxed fibers and did not changed much compared to rigor and active patterns. As a result, the $I_{1,1}/I_{1,0}$ ratio for the super-relaxing solution was 0.83 compared to 0.27 for the relaxed fibers. There was an ~1.5% shrinkage of the filament lattice when relaxed fibers went into rigor and a further ~0.5% shrinkage during active contraction. In the super-relaxing solution, the filament lattice expanded slightly, but remained shrunk compared to that in relaxed fibers (Fig. 2 *B*).

The intensity of A1 I_{A1} in rigor was used as a reference for the quantitative estimation of the fraction of myosin heads labeling the actin helix during active contraction at different temperature. For this reason, it was essential to check if this intensity remained unchanged after long-term activation during which muscle fibers were subjected to up to 50 double T-jumps and up to 35 s of x-ray exposure. In five experiments (different from those used for Figs. 1 and 2), the double T-jumps were repeated 10–15 times in rigor after 30–40 applications of the same protocol in active contraction. The off-meridional intensities obtained from these five fibers in rigor at the beginning and at the end of the experiments and during active contraction at 5–6°C are plotted against the meridional spacing in Fig. 3. To compare the intensities quantitatively, the patterns from the five fibers were summed after correction for the exposure in

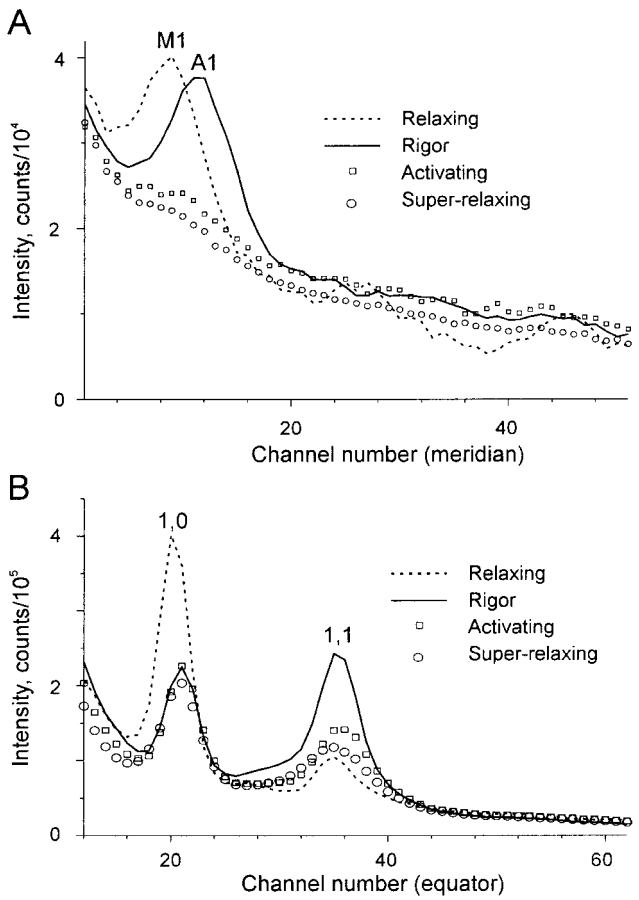

FIGURE 2 One-dimensional intensity profiles for the diffraction patterns from nine frog muscle fibers in the different states shown in Fig. 1. (*A*) The off-meridional intensity was integrated along the equator from (35 nm)$^{-1}$ to (8 nm)$^{-1}$ and plotted against the meridional spacing (0.013–0.079 nm)$^{-1}$. The area of integration is shown in the 2D diagram in Fig. 1. Layer lines M1 and A1 in the relaxed (*dashed line*) and rigor (*continuous line*) states, respectively, are labeled. The intensities in the activating (*squares*) and super-relaxed (*circles*) solutions are also shown. (*B*) the equatorial intensity profiles. The 1, 0 and 1, 1 reflections are labeled. One channel corresponds to (775.5 nm)$^{-1}$ in reciprocal space.

each state for each fiber and for the decay of the x-ray beam estimated by the ion chamber readings. The only difference in the intensity profiles between the rigor patterns collected from fresh fibers and the same fibers after 1–2 h of experiment was a decrease in the background. The reason for this decrease in the course of the experiment was an underestimation of the camera background scattering in the early stages of the experiments (see above). The position of A1 and its intensity I_{A1} remained the same within the 3% accuracy determined by the spatial resolution and noise. This shows that the A1 intensity is well preserved and not affected much by fiber run down. Therefore, I_{A1} in rigor seems to be a reliable reference for its value in other muscle states. It is worth mentioning that, during active contraction, the fiber background was higher than in rigor after contraction as one would expect from the decrease in the intensities of the layer line characteristics for contracting fibers (Fig. 3).

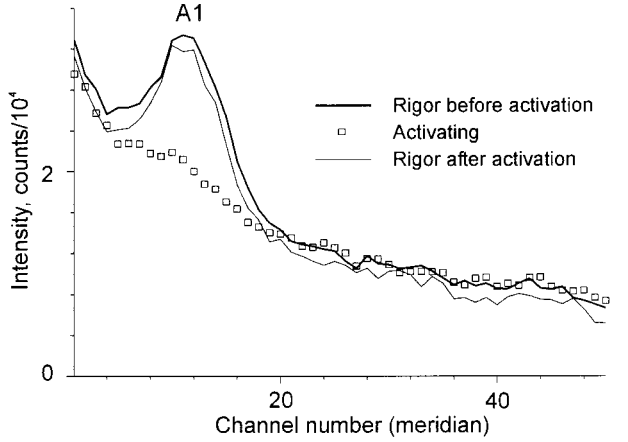

FIGURE 3 The off-meridional intensity profiles for five muscle fibers in rigor before activation (*bold line*), during active contraction (*squares*) and in rigor after activation (*thin line*). The area of integration was as in Fig. 2 *A*. Individual patterns were summed after correction for exposure of each fiber in each state and for the brightness of the beam as described in the Results section. These data were obtained from a set of five fibers different from those shown in Figs. 1 and 2.

Tension response to the double T-jump

The steady-state tension after the first and second T-jumps were 1.51 ± 0.05 fold (range 1.25 to 2.0) and 1.84 ± 0.08 fold (range 1.43 to 2.9) higher than that before the first T-jump (Mean ± SE, for 16 fibers), respectively. For fibers with low initial tensions at low-temperature, the fractional increase during the T-jump was higher than for fibers with high tensions at low-temperature. Following each T-jump (Fig. 4), tension rose by a process that was adequately described by a double exponential function (Bershitsky et al., 1997). The amplitudes of the two components were approximately equal. The rate constant of the first (fast) component was 730 ± 85 s^{-1} and 980 ± 100 s^{-1} after the first and second T-jumps, respectively. The rate constant of the second (slow) component was 76 ± 5 s^{-1} and 83 ± 8 s^{-1} for the jumps to ~17°C and ~30°C, respectively (Mean ± SE).

It should be noted that the duration of the T-jump in this series of experiments was set to 0.5–0.8 ms instead of 0.35 ms used earlier (Bershitsky et al., 1997). The slower temperature rise, achieved by using a lower peak current, reduced the risk of sparking between the fiber and the apparatus. Thus, the rate constant of the fast component of the mechanical response was perhaps underestimated.

Fiber stiffness at different temperature

To check whether the increase in force with temperature was due to recruitment of a higher number of cross-bridges interacting with actin, we measured fiber stiffness before and just after the T-jump protocol. For this, a 0.5% release–restretch cycle was applied to the fiber 200 ms before opening the shutter and 20 ms after its closing. Due to optical artifacts, it was difficult to measure changes in

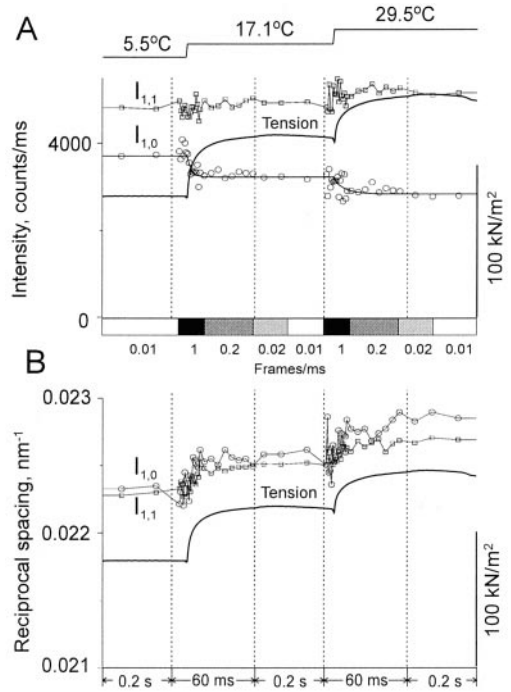

FIGURE 4 The time course of the changes in the (1, 0) and (1, 1) equatorial x-ray reflections during the double T-jump protocol. The intensities and spacing of the equatorial (1, 0) and (1, 1) x-ray reflections are shown in *A* and *B*, respectively. Temperature (*upper trace* in *A*) and tension (*thick lines* in *A* and *B*) are the average from 417 runs of the double T-jump protocol in 16 permeabilized frog muscle fibers. Figures above the temperature trace show the average temperature before and after the first and second T-jump. The vertical dashed lines show breaks in the time scale. (*A*) the intensities $I_{1,0}$ (*circles*) and $I_{1,1}$ (*squares*) of the equatorial reflections (1, 0) and (1, 1), respectively, were collected from the same 417 runs of the protocol. The abscissa corresponds to the center of the time intervals during which the x-ray data were collected. Gray scale and figures (frames/ms) in the bottom of *A* show the frequency of the x-ray framing at different time intervals of the protocol. The intensities in each time frame were estimated from the Gaussian fit of the peaks above a Pearson VII background and expressed as the number of photons per ms counted by the 2D detector. The Pearson VII function, $y(x) = h/\{1 + 4[(x - m)/w]^2(2^{1/S} - 1)\}^S$, has 4 parameters (*h*, *m*, *w*, and *s*); it becomes a Lorentzian at $s = 1$ and approaches a Gaussian when $s \to \infty$. The thin broken line connects the $I_{1,1}$ data points. The smooth line is an exponential fit through the $I_{1,0}$ data points with rate constants of $320 \pm 35\ s^{-1}$ and $136 \pm 28\ s^{-1}$ (Mean ± SD) for the first and second T-jump, respectively. (*B*) The positions of the (1, 0) and (1, 1) peaks are expressed in terms of the myosin–myosin distance, *d*, in the hexagonal lattice. The distance *d* was calculated using formulas $d = \sqrt{3}/2d_{1,0}$ and $d = 1/2d_{1,1}$ where $d_{1,0}$ and $d_{1,1}$ are the spacing of the (1, 0) and (1, 1) equatorial reflections. The results of the calculation of the *d* value using the $d_{1,0}$ and $d_{1,1}$ experimental data are shown in *B* by circles and squares, respectively.

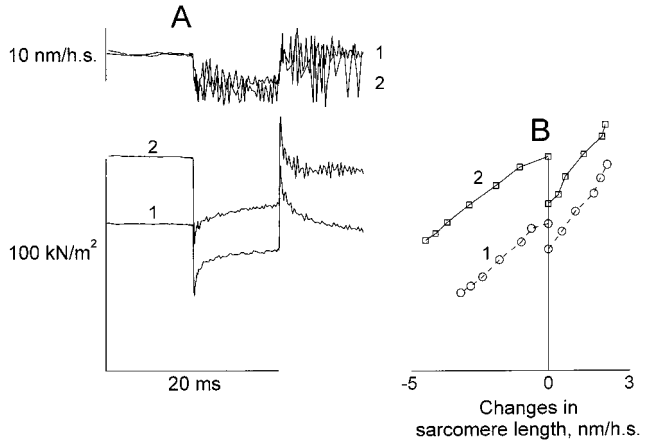

FIGURE 5 Stiffness of a contracting muscle fiber at the beginning and end of the double T-jump protocol. (*A*) tension transients initiated by the length step changes at 6°C (1) and 26°C (2) in an activated, partially cross-linked frog muscle fiber (*lower traces*). The length steps were applied 0.2 s before and 20 ms after the double T-jump protocol (Fig. 4) when the fiber was suspended in air. Upper traces are changes in sarcomere length in nanometers per half-sarcomere. Noise in the sarcomere length records is due to transverse fiber oscillations induced by the step length change. (*B*) Relationship between tension and sarcomere length during the steps. The tension calibration is as in (*A*).

sarcomere length when the length steps were applied to a fiber suspended in air. In some cases, however, the measurements were quite successful (Fig. 5). Although the length steps induced transverse oscillations of the fiber that initiated oscillations in the sarcomere length signal, these oscillations were relatively slow and did not detract from the measurement of the sarcomere length during the step itself (Fig. 5). These oscillations are usually less visible by the damping effect of surrounding water when the length steps are applied to fibers immersed in aqueous solutions. The slope for the relation between sarcomere length and tension during the steps at high temperature (26°C) was slightly less than that at low temperature (6°C). For stretches, the difference was not statistically significant: $2.9 \pm 8.2\%$ ($n = 7$), whereas for releases, the decrease in slope was significant: $16.1 \pm 4.9\%$.

Because the sarcomere length signal was not quite reliable for stiffness measurement in muscle fibers suspended in air, the effect of temperature on stiffness was also studied in four experiments for fibers in solution. Figure 6 shows a set of experimental records and the relation between sarcomere length and tension during stretches and releases of a muscle fiber in different solutions at different temperature. Because even slight EDC cross-linking partially switches on the regulatory proteins on the thin filaments (Bershitsky et al., 1996), the fibers produced substantial tension (20 to 45% of that at full activation at 2°C) and had a significant stiffness even in the absence of Ca^{2+} (Fig. 6). Both stiffness and tension were greatly reduced if the fibers were immersed in super-relaxing solution containing 50 mM BDM and 20 mM P_i that induced detachment of uncross-linked myosin heads from actin (Figs. 2 and 5, and Bershitsky et al., 1996). The curvature of the sarcomere length–tension diagram increased during the length step due to truncation of the tension responses induced by the fast partial tension recovery (Ford et al., 1977). This truncation was more pronounced at higher temperature (Fig. 6). To correct for the truncation, the steepest linear part of the diagram was used for the stiffness measurement as shown in Fig. 6 *B*. However, no correction was done for the intrinsic nonlinearity of the strain–stress diagram (Higuchi et al., 1995) that

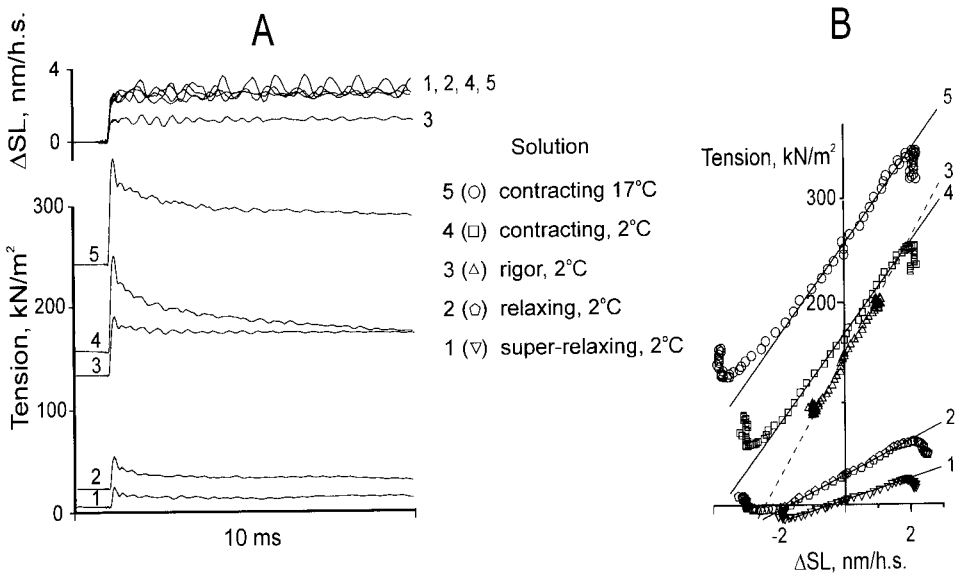

FIGURE 6 Stiffness of a muscle fiber measured with fast length changes in different solutions and at different temperature. (*A*) experimental records of changes in the sarcomere length (*upper traces*, in nanometers per half-sarcomere) and tension (*lower traces*). The traces were recorded from a muscle fiber in super-relaxing (1), relaxing (2), magnesium-free rigor (3), and activating solutions at 2°C (4) and 17°C (5). (*B*) plots of the changes in sarcomere length and tension during the step stretches and releases for the same muscle fiber. Data points were collected at a sampling rate of 125 kHz. Data for the stretches were obtained from the traces shown in (*A*). Straight lines are linear regression for the linear parts of the plots where the possible effect of truncation due to the finite duration of the steps was minimal. The dashed line corresponds to rigor stiffness.

only could lead to an underestimation of stiffness at low levels of tension, or, in our case, at lower temperature. After stiffness measurement at full Ca^{2+} activation at 2°C, the temperature was increased in 5°C steps, and stiffness was measured at each temperature. In two fibers, the changes induced by a temperature increase to 22°C were reversible, and tension and stiffness returned to their initial levels (within 5%) after cooling down to 2°C. In two other fibers, the increase in tension with temperature induced some irreversible damage at 17°C and 22°C so that tension at 2°C decreased to <85% of the initial level. Only measurements, where reversible changes in tension and stiffness induced by temperature shifts from 2°C to 12°C and to 17°C were obtained, were used for the analysis.

Figure 7 summarizes the results of the tension and stiffness measurements in all four muscle fibers used in this series. When active force was decreased by using Ca^{2+}-free solution and decreased further by adding BDM and P_i,

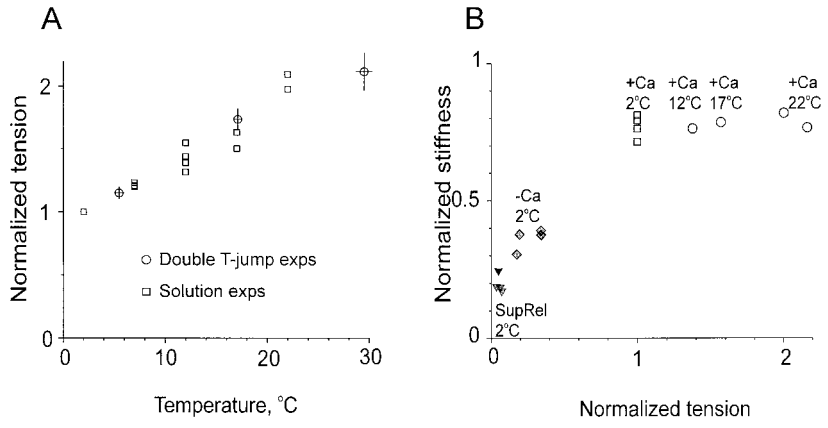

FIGURE 7 Normalized tension and stiffness of muscle fibers in different conditions. (*A*) tension − temperature relation in fully activated frog muscle fibers. Squares represent data obtained in four experiments in solution; circles refer to average data for the double T-jump experiments. The error bars show the standard error of the mean ($n = 16$). Tension for each fiber was normalized for that at 1–2°C. (*B*) All data obtained from four experiments with fibers in the activating solution, including that presented in Fig. 6, are shown. Stiffness in the super-relaxing solution at 2°C (SupRel, *triangles*), in the relaxing solution (−Ca, *diamonds*) and in the activating solution at 2°C (+Ca, *squares*) and, at higher temperature (+Ca, *circles*), are shown against tension normalized for that during active contraction at 2°C. The temperature of the activating solution is shown above the data points. Stiffness was measured from the slope of the linear regression lines as shown in Fig. 6 and normalized for that in magnesium-free rigor solution at 2°C.

stiffness decreased with tension in a linear manner (Fig. 7 *B*). About 20% of rigor stiffness remained in the super-relaxing solution due to a contribution of the myosin heads covalently cross-linked to actin with EDC and perhaps some attached uncross-linked heads. However, the substantial increase in active tension with temperature at full Ca^{2+} activation was not accompanied by any measurable increase in stiffness. This was shown by the fact that the slope of the stiffness–temperature relation was (1 ± 1)% per 10°C (n = 4), i.e., it was not different from zero. Rigor tension and stiffness decreased slightly with temperature as described by Bershitsky and Tsaturyan (1986, 1989). However the decrease in rigor stiffness was smaller, (2.3 ± 4.6)% per 10°C, if the change in sarcomere length, rather than that of the total fiber length, was used for the stiffness measurement. Taking into account the significant scatter in the data for these small changes in stiffness, we conclude that stiffness remained constant within a 5% error when the force increased by nearly two-fold with temperature.

Time course of the (1, 0) and (1, 1) equatorial x-ray reflections

As shown in Fig. 4 *A*, the tension rise induced by the T-jumps was accompanied by a substantial decrease in the intensity of the (1, 0) equatorial reflection ($I_{1,0}$) and a small increase in the intensity of the (1, 1) reflection ($I_{1,1}$). The changes in $I_{1,0}$ were not instantaneous, but faster than the increase in tension. At ~17°C and ~30°C, $I_{1,0}$ decreased by a factor of 0.85 and 0.74, respectively, compared to the intensity at ~5°C, whereas $I_{1,1}$ increased only by a factor of 1.04 and 1.07. The time resolution and the signal–noise ratio did not allow determination of whether the changes in $I_{1,0}$ were simultaneous with the fast component of the tension rise or slower, but these changes were overall faster than the tension rise and were largely complete ~10 ms after the T-jumps (Fig. 4 *A*). The noise in the data is photon noise and corresponds to the square root of the total number of counted photons before subtraction of the background. The background intensity under the equatorial reflections is approximately 3 times the intensity in the (1, 0) and (1, 1) peaks.

The positions of the (1, 1) and (1, 0) equatorial reflections shifted away from the meridian when tension increased after the T-jumps (Fig. 4 *B*), indicating some shrinkage of the filament lattice. Expressed in terms of the size, d, of a cell in the hexagonal filament lattice (or myosin-to-myosin distance), this shift was equivalent to a ~1.5% shrinkage of the fiber lattice when temperature increased from ~5 to ~30°C. The time course of shrinkage was approximately synchronous with the tension rise.

Time course of the meridional x-ray intensity of the 3rd myosin layer line M3

Figure 8 *A* shows the time course of the change in the intensity of the meridional reflection on the M3 (I_{M3}). At

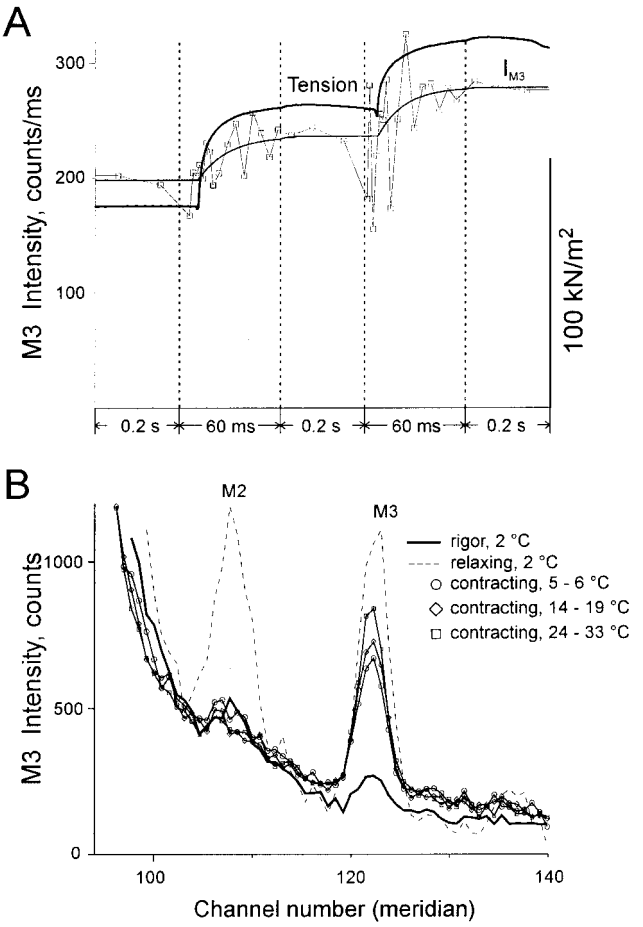

FIGURE 8 Changes in the intensity of the M3 meridional reflection during the double T-jump protocol. (*A*) the time course of the intensity I_{M3} (*squares*) of the M3 meridional reflection at ~(14.5 nm)$^{-1}$ during the protocol. The data just before and after the T-jumps are shown at 2-ms time resolution. The vertical dashed lines show breaks in time scale. The smooth line is an exponential fit through the I_{M3} data points with rate constants of 56 ± 21 s^{-1} and 65 ± 50 s^{-1} (Mean ± SD) for the first and second T-jump, respectively. The tension trace and the 2D diffraction data used are the same as those in Fig. 4. The intensity in the M3 meridional diffraction peak was integrated after Pearson VII background subtraction and expressed as the number of photons per ms counted by the 2D detector. (*B*) Meridional intensity profiles in rigor (*bold line*), during relaxation (*dashed line*), and active contraction at the lower (5–6°C, *circles*), intermediate (14–19°C, *diamonds*) and higher (24–33°C, *squares*) temperatures are plotted against the meridional spacing. No background subtraction was done. The positions of M2 and M3 are labeled.

~17°C and ~30°C, I_{M3} was higher than that at 5–6°C by factors of 1.2 and 1.41, respectively. The photon noise prevented the time course of the changes in I_{M3} to be determined with a high time resolution. As shown in Fig. 8 *A*, the changes in I_{M3} probably accompanied the slow component of tension rise. The profiles of the meridional x-ray intensity in the region of M2 and M3 myosin layer lines are shown in Fig. 8 *B*. The intensity of the M3 meridional reflection changed with temperature, but not its width along the meridian. The changes in the equatorial width of the M3 reflection were also less than 10% (data not shown). The spacing of the meridional M3 reflection in contracting

muscle was different from that in relaxed and rigor states (Huxley and Brown, 1967; Bordas et al., 1993), but, in contracting muscle, it did not depend on temperature, at least within the spatial resolution of our experiments (Fig. 8 *B*).

2D diffraction patterns at different temperature

Figure 9 shows the 2D diffraction patterns obtained by summing the patterns obtained from each of 16 fibers in a total of 417 runs of the double T-jump protocol. The myosin layer lines are clearly seen in the relaxed pattern, and the actin layer lines are seen in the rigor pattern. We found no difference in the rigor diffraction patterns collected before and after EDC cross-linking: the spacing and the intensity of the main equatorial and meridional reflections, as well as of A1 and A6, were the same within the accuracy of our experiments and taking into account the 3% decay in beam intensity during the experiment.

During active contraction, all the layer lines, except the meridional spot on M3 at $\sim(14.5\ \text{nm})^{-1}$ and A6 and A7 at $\sim(5.9\ \text{nm})^{-1}$ and $\sim(5.1\ \text{nm})^{-1}$ became very weak and almost invisible. The M3 meridional spot was more intense during contraction than in rigor, whereas the A6 and A7 were brighter than in relaxed muscle fibers, but less bright than in rigor (see also Fig. 8 *B*). These features of the active diffraction pattern show that, during contraction, most of the cross-bridges do not label effectively either the myosin or the actin helices while they retain a $\sim(14.5\ \text{nm})^{-1}$ periodicity along the myosin filaments. An increase in the inten-

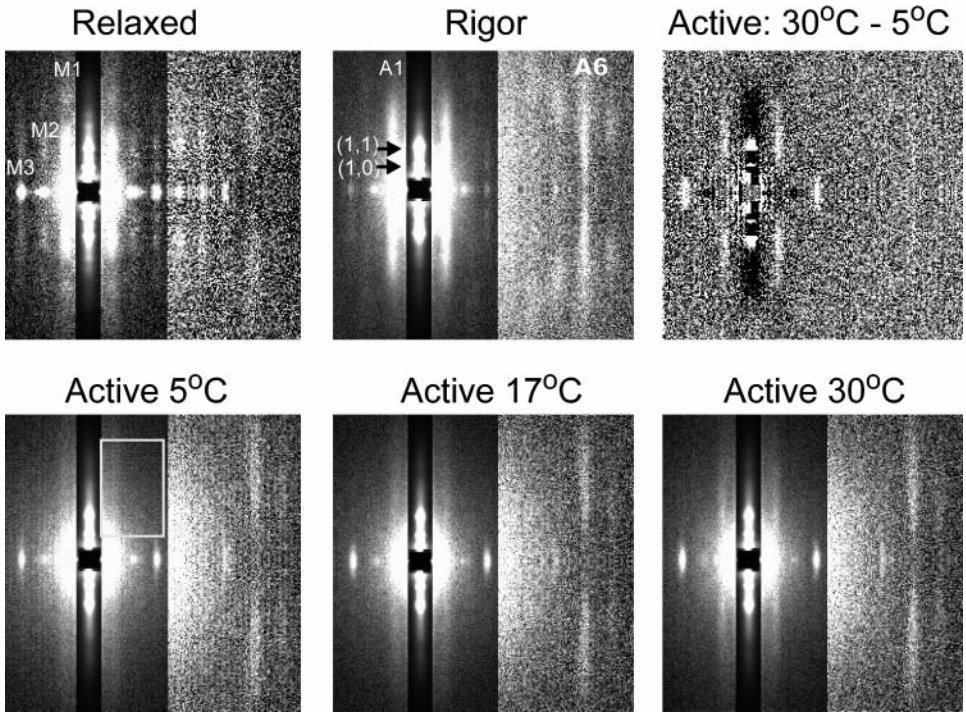

FIGURE 9 2D x-ray diffraction patterns from frog muscle fibers at different temperatures. The x-ray diffraction patterns from 16 permeabilized frog muscle fibers in the relaxed state, in rigor, and at the plateau of active isometric contraction at 5–6°C, 14–19°C, and 24–33°C are shown. Higher intensity is shown as white and the equator is vertical, and digitally attenuated 20-fold to scale the intensity of the equatorial reflections onto the same gray-scale as for the weaker reflections. The inner parts of the patterns from the equator up to a meridional spacing of $\sim 0.08\ \text{nm}^{-1}$ was digitally attenuated by a factor of 5 for the same reason. The first two patterns in the top row show the relaxed and rigor patterns at 5–6°C obtained before activation. The bottom row shows the patterns obtained during the plateau of isometric tension after activation at each of the three temperatures. The top right pattern is the difference between the active diffraction patterns at the higher (~30°C) and lower (~5°C) temperature. The threshold in the top right pattern was decreased compared to others to make small changes more visible. The upper and lower halves of each pattern were symmetrically averaged. The active patterns were obtained during 417 runs of the double T-jump protocol in 16 fibers (8 to 50 runs per fiber) and added together. The patterns were collected during the 0.2-s plateaus of contraction at each of the three temperatures (Fig. 4). The relaxed patterns for each fiber were collected during 1-s exposure soon after mounting the fiber in the experimental set-up. The relaxed patterns from each fiber were normalized by scaling for the total time of fiber exposure during 0.2-s active contractions and the beam intensity and then added together. The rigor pattern was obtained during 5-s exposures to the x rays of each of 16 fibers after EDC cross-linking, but before the fibers were activated. Then 16 patterns were normalized and added together using the same procedure as that described for relaxed patterns. Total exposure was 83.4 s for the active contraction at each of three temperatures, 16 s during relaxation, and 80 s in rigor. The main equatorial reflections, (1, 0), (1, 1), the myosin M1–M3 and the actin A1 and A6 layer lines are labeled. A rectangle shows the area of integration used for the off-meridional intensity profiles presented in Figs. 10 and 11. Light and dark vertical lines seen in the lower left and upper right panels are due to a nonphoton noise induced by the wire-to-wire modulation in the electronics of the 2D detector. There are 200 vertical and 200 horizontal wires in the detector, and its spatial sensitivity is modulated by these wires. When the detector electronics warmed up after it started to count the photons, the phase of the modulation changed with time and became stable in a few tenths of a second and then the noise could be effectively corrected by dividing with the detector response (see Methods). Unfortunately, this correction was not effective in the earlier time frames before the first T-jump.

sities of A6 and A7 indicates that myosin cross-bridges probably bind to actin monomers. There is also a remainder of the 1st actin/myosin layer line at $(36-43\ \text{nm})^{-1}$ which is more visible at the higher temperature. An increase in the x-ray diffraction intensity in the off-meridional part of the pattern near A1 as well as an increase in I_{M3} described above are clearly seen in the differential diffraction pattern (Fig. 9, *top right panel*).

Intensity of M1 and A1

Fig. 10 shows the meridional profiles of the off-meridional x-ray diffraction intensity from relaxed, rigor, and active muscle fibers at 5–6°C and ~30°C. The region of radial integration of $(35\ \text{nm})^{-1}$ to $(8\ \text{nm})^{-1}$ shown in Fig. 9 was chosen because it contains most of the intensity of A1 and M1 where the cross-bridges could contribute (Yagi, 1991). The peaks in the relaxed and rigor patterns were considered as pure M1 and A1, respectively, because all cross-bridges are detached from actin in relaxed muscle and strongly bound in rigor (Cooke et al., 1984; Lovell et al., 1981). The A1 and M1 peaks in rigor and relaxed fibers were fitted with Gaussians above a Pearson VII background (see Fig. 4). The total intensities of the M1 peak from relaxed fibers and the A1 peak from the same fibers in rigor differ by only 2.7%.

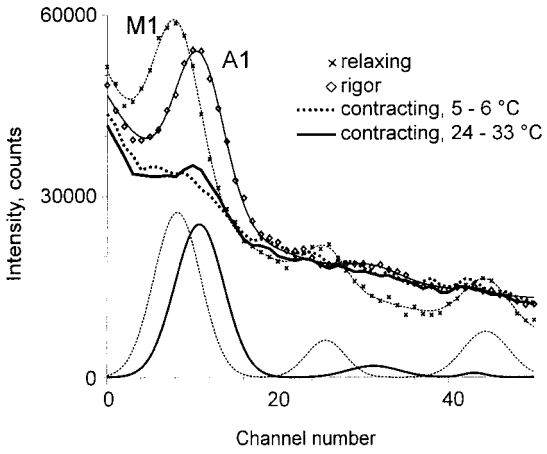

FIGURE 10 The intensity of the first layer line. The intensity of the layer line in the relaxed state (*crosses*), in rigor (*diamonds*), and during contraction at 5–6°C (*dotted line*) and at 24–33°C (*bold line*) was obtained by radial integration from $(35\ \text{nm})^{-1}$ to $(8\ \text{nm})^{-1}$ of the 2D diffraction patterns shown in Fig. 9. The intensity of the first layer line in relaxed (*dashed line*) and rigor (*continuous line*) states was fitted with a sum of three Gaussian peaks above Pearson VII background. The peaks without the background are shown at the bottom of the plot. The first peaks for the relaxed and rigor fibers were considered as M1 and A1, respectively. Their positions and widths were used for extraction of the M1 and A1 components from the first layer line during active contraction at different temperature. The total intensity of A1 in rigor was 97.3% of that of M1 in relaxed fibers. Note that the background around the first layer line is lower during contraction at higher temperature than at lower temperature and that the position of the peak on the first layer line at ~30°C is close to that in rigor while its amplitude increases with temperature. Two other peaks are M2 and M3 for relaxed fibers and A2 and M3 for fibers in rigor. One channel corresponds to $(775.5\ \text{nm})^{-1}$ in reciprocal space.

It is seen that, in contracting fibers, the intensity of the 1st layer line increases with temperature and its spacing shifts closer to that of A1 in rigor. The background level decreases with increasing temperature, indicating that the cross-bridges become better ordered.

During active contraction, the peak in the region of the 1st layer line is a mixture of the A1 and M1 components (Huxley et al., 1982; Yagi, 1991). These peaks at three different temperatures were fitted by a weighted sum of the A1 and M1 Gaussians so that only the relative amplitudes of the peaks and the background level varied during the fit while the positions and widths of the Gaussians were fixed. By doing this, we determined the relative contribution of the A1 and M1 to the mixed A1/M1 layer line at each temperature. For each pattern, the background was approximated by a Pearson VII function (Fig. 11). Quantitative results are presented in Table 1. When tension increased with temperature, the contribution of A1 increased while the contribu-

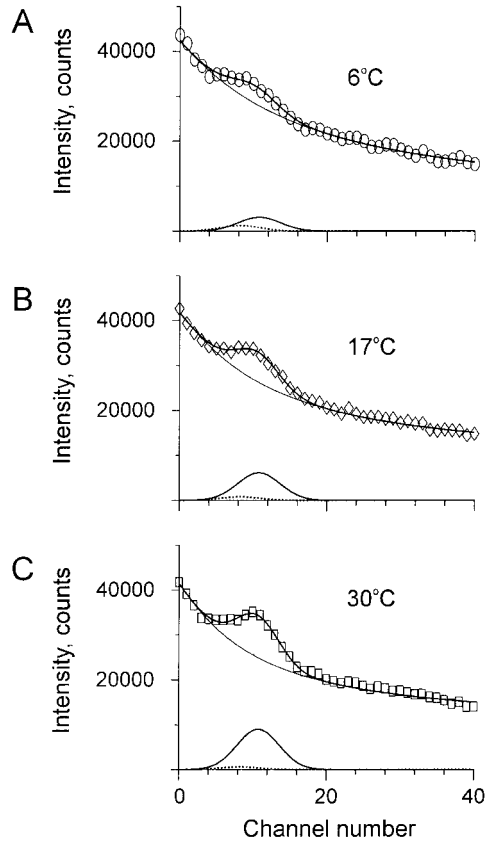

FIGURE 11 Contributions of the M1 and A1 components to the first layer line during active contraction at different temperature. The intensities of the first layer line during contraction at ~5–6°C (*A, circles*), ~17°C (*B, diamonds*), and at ~30°C (*C, squares*) were fitted with a weighted sum of the M1 and A1 components above Pearson VII background. The positions of the peaks and the widths of the M1 and A1 components were taken from the relaxed and rigor data (Fig. 10) so that only the amplitudes of the peaks varied during the fit. The fit and the background are shown as continuous lines. Dashed and bold lines in the bottom show the M1 and A1 components, respectively, after background subtraction. The intensities of the first layer line were obtained by the same integration of the 2D patterns as those in Fig. 10. One channel corresponds to $(775.5\ \text{nm})^{-1}$ in reciprocal space.

TABLE 1 Relative contribution of the A1 actin and M1 myosin layer lines in the first layer line in the x-ray diffraction pattern from actively contracting frog muscle fibers at different temperature

State	M1 layer line (%)	A1 layer line (%)
Rigor	0	100
Relaxation	100	0
Contraction at ~5.5°C	4.6	12.1
Contraction at ~17°C	2.8	24.2
Contraction at ~29.5°C	2.2	35.6

tion of M1 remained small. This indicates that the increase in force generation is accompanied by an increase in the number of myosin cross-bridges labeling the actin helix.

The radial distribution of the x-ray diffraction intensity along the A1 component of the 1st layer line during contraction at ~30°C is shown in Fig. 12. The distribution is similar to that in rigor but ~2.8 times less intense. The only difference is a small off-meridional shift. The intensity of the A1 component at low temperature and the intensities of the M1 component at all three temperatures were too weak to allow measurement of their radial distributions with any reasonable accuracy.

Intensity of A6

The data collected were too noisy for measuring the time course of temperature-induced changes in the intensity of A6 in the 2D diffraction patterns. Nevertheless the intensity profiles obtained by integration across A6 were good enough to visualize some shift of the peak of the intensity toward the meridian at elevated temperature (Fig. 13). This meridional shift is typical for rigor diffraction patterns (Huxley and Brown, 1967; Wakabayashi and Amemiya, 1991).

At 30°C, the intensity of A6 in the active fibers was 82.5% of that in rigor. The total intensity of A6 increased by only ~17% when tension rose by a factor of 1.84 with a temperature change from 5°C to 30°C in active fibers. The data, at 17°C and especially at 5–6°C, where the wire-to-wire modulation in the detector was apparent (Fig. 9), were too noisy for accurate quantitative measurement.

Response of muscle fibers in the rigor state to double T-jump

To check that the temperature-induced changes in the x-ray diffraction pattern during contraction are specifically linked to force generation, and not to temperature itself, the double T-jump protocol was applied to fibers in rigor. Figure 14 shows that, in this case, an increase in temperature led to an instantaneous tension drop followed by a small and slower tension rise. This tension drop is due to the thermal expansion of the fiber (Bershitsky and Tsaturyan, 1985, 1989; Goldman et al., 1987; Davis and Harrington, 1987). The equatorial intensities $I_{1,0}$ and $I_{1,1}$ increased by 1.2% and decreased by 1.1%, respectively, when temperature increased from 5–6°C to ~30°C (Fig. 14 *B*). The filament lattice shrunk by ~0.5% at the higher temperature judging from the positions of peaks of the (1, 0) and (1, 1) equatorial reflections. The intensity of A1 did not change with temperature with the accuracy of our measurements. More pronounced changes were observed in the meridional part of

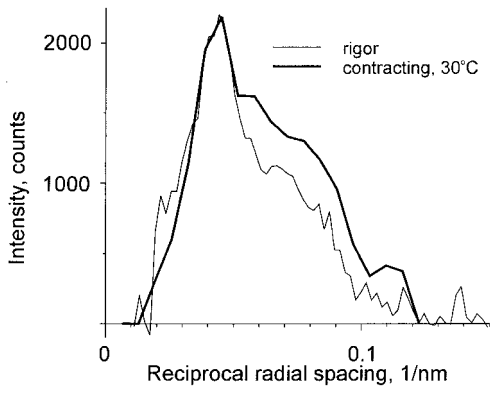

FIGURE 12 Equatorial distribution of the intensity along A1. The distribution of the x-ray diffraction intensities along A1 in rigor (*thin line*) and during active contraction at ~30°C (*bold line*) are shown. The rigor intensity was attenuated 2.8 times for easier comparison of the shapes. The intensity in rigor was obtained by fitting the layer line with the A1 peak above Pearson VII background for each equatorial position so that the meridional spacing and the width were fixed. The A1 component of the first layer line during active contraction was obtained by decomposition of the intensity by the M1 and A1 components as described in the legend for Fig. 11, but 5-pixel-wide slices were integrated along the equator and then used for the fit to reduce noise. The intensities of the M1 component at ~30°C, as well as the intensities of the M1 and A1 components at 5–6°C, were too noisy to determine their radial distributions. Zero on the abscissa marks the position of the meridian.

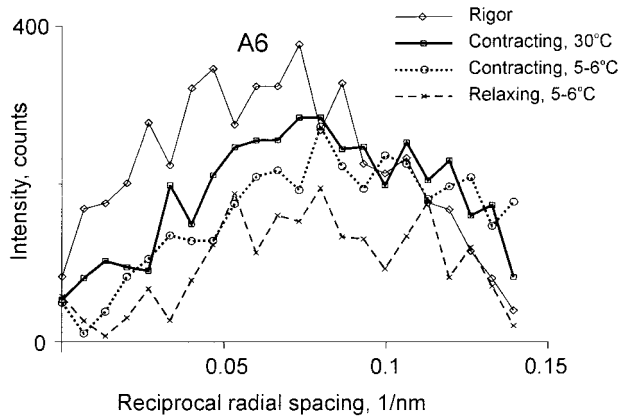

FIGURE 13 Equatorial distribution of intensity in the A6. Intensity distribution along A6 at ~$(5.9\ \text{nm})^{-1}$ during relaxation (*crosses*, *dashed line*), in rigor (*diamonds*, *thin line*), and during active contraction at the lower (5–6°C, *circles*, *dotted line*) and higher (24–33°C, *squares*, *bold line*) temperature. The data points were obtained by integration of the 2D diffraction pattern across the layer line, linear background subtraction and averaging over five data points along the equator to reduce noise. Zero on the abscissa marks the position of the meridian.

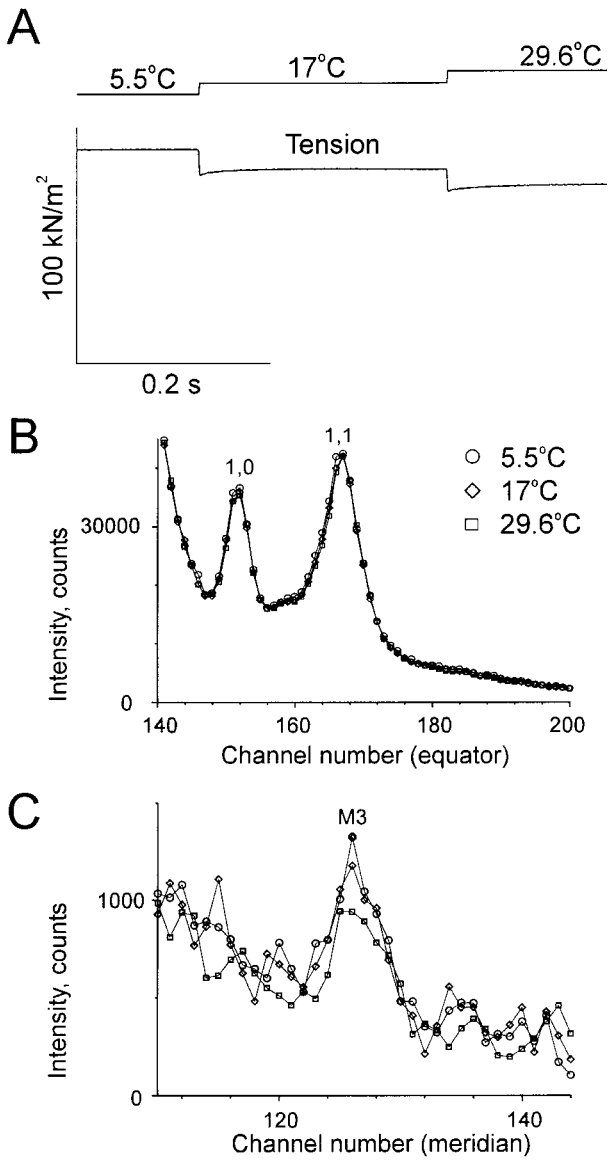

FIGURE 14 Mechanics and structural changes in the double T-jump protocol in rigor. Temperature and tension (*A*) are averaged from 60 runs of the protocol in five frog muscle fibers. The equatorial (*B*) and meridional (*C*) x-ray intensities at the lower (5–6°C, *circles*), intermediate (14–19°C, *diamonds*), and higher (24–33°C, *squares*) temperature were collected for 12 s at each temperature and plotted against equatorial (*B*) and meridional (*C*) channel number. One channel corresponds to $(775.5\ \text{nm})^{-1}$ in reciprocal space.

M3 (Fig. 14 *C*). A decrease in M3 intensity is clearly seen. Note that in rigor, the temperature-induced changes in M3, (1, 0), (1, 1) intensities and tension were all in the opposite direction from those in active muscle (Figs. 4 and 8).

Equatorial intensities during contraction at sub-maximal activation

To compare changes in the equatorial x-ray intensities induced by an increase in temperature during isometric contraction at full activation with those in which tension changes are the result of a variation in the number of myosin cross-bridges involved in the interaction with actin, the effect of Ca^{2+} on the $I_{1,0}$ and $I_{1,1}$ intensities was studied in five fibers. After rigorization and EDC cross-linking, fibers were immersed alternately in the activating and relaxing solutions, and the x-ray diffraction patterns were collected during 2.5-s-long exposures in air at 5–6°C. Total exposure was 10–20 s in each state for each fiber. Due to the alternate exposures, the effects of deterioration of the fiber and of the x-ray beam were approximately the same in the presence and absence of Ca^{2+}. Tension produced in the absence of Ca^{2+} was (33 ± 3)% of that at full activation as the regulatory proteins were partially activated by EDC cross-linking (Bershitsky et al., 1996). In the presence of Ca^{2+}, $I_{1,0}$ was (71 ± 4)% lower and $I_{1,1}$ was (117 ± 3)% of those at submaximal activation. These changes are different from those observed when tension increases with temperature at full activation (Fig. 4): in that case the increase in $I_{1,1}$ was small.

DISCUSSION

The main result of the experiments presented here is that an increase in temperature leading to a considerable increase in tension (without any visible change in stiffness) is accompanied by substantial changes in the x-ray diffraction pattern, namely, a decrease in the intensity of the (1, 0) equatorial reflection; an increase in the off-meridional intensity of A1 and in the meridional intensity of M3 and a shift of the intensity peak of A6 toward the meridian. These changes are interpreted in terms of possible structural changes responsible for force-generating transition in myosin cross-bridges attached to the thin filaments. Possible artifacts and alternative explanations are discussed below.

Possible artifacts and recruitment of cross-bridges

Structural changes following the T-jumps might result from a recruitment of detached cross-bridges into states where they interact with actin and thus cause force generation. Stiffness measurements before and after the double T-jump protocol (Fig. 5) show that stiffness estimated from the slope of the sarcomere length–tension diagram decreased with temperature. More careful stiffness measurements of muscle fibers in the solution trough (Figs. 6 and 7) show, however, that stiffness changes with temperature by $<5\%$ per 10°C. In the worst case, a hypothetical increase in stiffness with temperature in the range of 5.5 to 29.5°C could be $5\% \times (29.5°C - 5.5°C)/10°C = 12\%$. Taking into account the compliance of the thin and thick filaments (Suzuki and Sugi, 1983; Huxley et al., 1994; Wakabayashi et al., 1994; Linari et al., 1998; Dobbie et al., 1998), the number of the cross-bridges attached to actin could increase by 20% if stiffness increased by as much as 12%. Even with this worst case estimation, the possible change in stiffness is

too small to account for the 1.84-fold increase in force with temperature if force is proportional to the number of attached cross-bridges as revealed by the stiffness measurements. Most probably, the number of cross-bridges attached to the thin filaments remained constant within ±10%, so that changes in the x-ray diffraction intensities observed at the higher temperature were mainly due to conformational changes in the cross-bridges attached to actin.

The changes in the x-ray diffraction pattern with temperature also provide evidence that recruitment of detached cross-bridges does not account for the observed changes. When activated frog muscle fibers run out of ATP and all cross-bridges become attached to actin (Bershitsky et al., 1996, 1998), $I_{1,0}$ decreases only slightly (by ~15%), whereas $I_{1,1}$ increases much (by a factor of 1.5–2). The intensities of the equatorial reflections following increases in temperature in activated fibers changed in the same direction, but were very different quantitatively. At ~30°C $I_{1,0}$ decreased by 26%, whereas $I_{1,1}$ increased only by 7% (Fig. 4) compared to their values at 5–6°C. Also, the time course of the changes in $I_{1,0}$ was faster than the overall increase in tension after the T-jumps and appears to follow the fastest component of tension rise (Fig. 4), whereas cross-bridge reattachment in both frog and rabbit muscle fibers takes place more slowly and follows the slow component of tension rise (Tsaturyan and Bershitsky, 1988; Bershitsky and Tsaturyan, 1992). At submaximal activation, tension is proportional to the number of attached cross-bridges judging from stiffness measurements (Fig. 6) and taking into account the compliance of the thin and thick filaments (Huxley et al., 1994; Wakabayashi et al., 1994; Linari et al., 1998; Dobbie et al., 1998). Changes in the number of attached cross-bridges affect both $I_{1,0}$ and $I_{1,1}$ in the same proportion (Yu et al., 1979; Brenner and Yu, 1985). This is in contrast to the changes with temperature at full activation where $I_{1,1}$ remains nearly constant while $I_{1,0}$ decreases. Both stiffness and equatorial changes make it unlikely that the main reason for the structural changes and force generation following the T-jumps is recruitment of detached cross-bridges.

Experiments with fibers in rigor (Fig. 14) show that the T-jump itself does not produce the structural changes observed during activation. The intensity of the M3 meridional reflection, I_{M3}, decreased at the higher temperature in rigor (Fig. 14), whereas it increased during active contraction (Fig. 8). The decrease in I_{M3} in rigor was probably caused by temperature-induced decrease in tension (Bershitsky and Tsaturyan, 1985, 1989; Goldman et al., 1987; Davis and Harrington, 1987), because, when a rigor fiber is stretched, I_{M3} increases (Bershitsky et al., 1996; Dobbie et al., 1997). Thus, the changes in the x-ray diffraction pattern following the T-jumps in actively contracting muscle fibers were associated with changes in orientation and/or shape of the myosin heads, not with a temperature effect per se. I_{M3} changed in the same direction as tension, regardless of the state of the fiber or of the method used to change tension, whether it was achieved by varying the extent of activation, temperature, or fiber length, in both active or rigor states.

The exhaustion of ATP or ADP accumulation during the relatively long contraction of fibers suspended in air may cause some changes in the x-ray diffraction pattern, particularly at the higher temperature. To avoid this problem, we used a high concentration of phosphocreatine and chicken creatine phosphokinase with a high specific activity (Bershitsky et al., 1996). The time course of changes in $I_{1,0}$ and $I_{1,1}$ did not show signs of ATP depletion. The changes in $I_{1,0}$ were fast and complete in 10–15 ms, whereas the intensities of both equatorial reflections remained constant on a slower time scale when effects of changes in ATP or ADP concentrations were expected. So, it is unlikely that changes in the x-ray diffraction pattern were due to changes in concentration of substrate or products of the ATPase reaction.

Comparison with previous data

The absence of temperature-induced changes in the equatorial x-ray intensities in rigor (Fig. 14) agrees with the observations of Rapp and Davis (1996), who also did not see changes unless temperature was increased to >50°C where dramatic disorder of the filament lattice was induced. The highest temperature in our experiments was 33°C to avoid gross damage to the mechanical and structural properties of muscle fibers. The results of the experiments presented here are in good agreement with those reported earlier (Bershitsky et al., 1997). The increase in temperature from 5–6°C to 20.5 ± 1.5°C (after recalibration of the temperature jump instrument, see Methods), induced tension to increase 1.68 times (Bershitsky et al., 1997). This figure is in keeping with the results shown here where T-jumps to 17.1°C and 29.5°C induced tension to rise 1.51 times and 1.84 times, respectively. Changes in the $I_{1,0}$, $I_{1,1}$ equatorial and I_{A1} intensities reported by Bershitsky et al. (1997) are also intermediate between those found here after the first and second T-jumps in the double T-jump protocol (Figs. 4 and 10; Table 1). The only difference is that an increase in the I_{M3} meridional intensity in earlier experiments was about 6% (Bershitsky et al., 1997), significantly less than that found now, 20 and 41% for increases to ~17 and ~30°C, respectively (Fig. 8). Possible reasons for this difference will be discussed later.

Equatorial intensities

The increase in force induced by the T-jumps was accompanied by a fast and substantial decrease in $I_{1,0}$ and a small increase in $I_{1,1}$ (Fig. 4). At ~30°C, $I_{1,0}$ was 26% less intense, whereas $I_{1,1}$ was only 7% brighter than at 5–6°C. Thus, force generation is accompanied by a significant radial and/or azimuthal movement of myosin cross-bridges. As we argued above, this movement is unlikely to be just an increase in the number of myosin cross-bridges attached to actin, because, in this case, one would expect much higher

changes in $I_{1,1}$ than in $I_{1,0}$ (Yu, et al., 1979; Brenner and Yu, 1985). It was suggested (Harford and Squire, 1992; Brenner and Yu, 1993) that changes in the equatorial intensities similar to those described here could result from a transition of myosin cross-bridges attached to actin weakly and nonstereo-specifically to a strongly (i.e., stereo-specifically) bound state in which orientation of a myosin cross-bridge in space is fully determined by the orientation of the actin monomer to which it binds.

The terms "weak" and "strong" binding refer to the affinity of the myosin heads to actin observed in experiments with solubilized muscle proteins and protein fragments, and do not relate directly to the mechanical and structural properties of the cross-bridges. We shall use the terms "nonstereo-specific" and "stereo-specific" binding to confer structural and mechanical meaning to the terms weak and strong binding, respectively, as follows. The nonstereo-specifically bound myosin heads are able to rotate with respect to the site of electrostatic contact between actin and S1 (Rayment et al., 1993). The stereo-specifically bound myosin heads have restricted rotation, presumably because of the tighter binding to actin brought about by an increase in the myosin–actin contact area. For this reason, we propose that the C-terminals (S1-S2 junctions) of the nonstereo-specifically bound heads remain in close proximity to their relaxed positions on the three-stranded helix on the surface of the myosin rod while the weak actin binding sites are attached to the thin filaments. So, these cross-bridges form a halo around the thick filaments. In contrast, the stereo-specifically bound cross-bridges form a halo around the thin filaments as they are incorporated into the actin helix (Malinchik and Yu, 1995).

To simulate the effect of a transition from the nonstereo-specific to the stereo-specific binding on the $I_{1,0}$ and $I_{1,1}$ equatorial x-ray intensities, we used a mathematical model proposed by Malinchik and Yu (1995). The result of the modeling is shown in Fig. 15. When the cross-bridges rearrange from a halo surrounding the thick filaments to a halo surrounding the thin filaments, $I_{1,0}$ decreases significantly while $I_{1,1}$ increases very slightly. The low sensitivity of $I_{1,1}$ to the transition to the stereo-specifically bound state can be explained by the fact that the total electron density of the (1, 1) planes does not change much. In contrast, the electron density near the thick filament backbone decreases when more cross-bridges contribute to the actin halo. This leads to a decrease in $I_{1,0}$ as the electron density in the (1, 0) planes decreases. $I_{1,0}$ also decreases because an increase in the scattering power of the thin filaments leads to a decrease in contrast of the (1, 0) planes as more of the cross-bridge mass is spread between the (1, 0) planes. In summary, changes in the $I_{1,0}$ and $I_{1,1}$ intensities after the T-jumps agree well with the results of the modeling based on the assumption that the tension rise following the T-jump is accompanied by a transition of nonstereo-specifically attached cross-bridges to a stereo-specific bound state while the total number of cross-bridges interacting with actin remains constant.

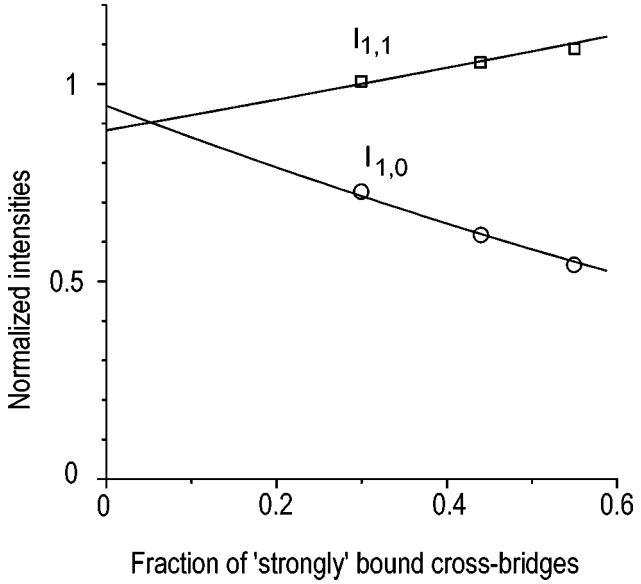

FIGURE 15 The results of mathematical modeling of the effect of the transition from nonstereo-specific to stereo-specific binding state on the equatorial x-ray intensities $I_{1,0}$ and $I_{1,1}$. The model suggested by Malinchik and Yu (1995) was used. Cross-bridges nonstereo-specifically attached to actin were assumed to form a uniform halo surrounding the thick filaments, whereas stereo-specifically bound cross-bridges form a uniform halo around the thin filaments. Myosin to myosin distance and radii of the thick and thin filaments of 42 nm, 8 nm, and 4.5 nm, respectively, were taken. The width of the cross-bridge halos around the thin and thick filaments were 12 nm, and the electron density of the halos was assumed uniform in radial and azimuthal directions. The root mean square of isotropic displacement of the thick and thin filaments from their positions in a perfect hexagonal lattice (Malinchik and Yu, 1995) was taken as 4 nm and 2.5 nm, respectively. The relative weights of the backbones of the thick and thin filaments were 36 and 16, while the total weight of the halo within a hexagonal unit cell was 20. The last figure is less than the total relative weight of myosin cross-bridges (~33 units, Malinchik and Yu, 1995), but we assumed that not all cross-bridges, only 60% of them, are attached to actin during isometric contraction and that detached cross-bridges do not contribute to the Bragg reflections, but only to a diffuse background scattering. When the percentage of the strongly bound cross-bridges increased, the mass of the actin-based halo increased while the mass of the myosin-based halo decreased, so that the total mass of 20 units remained constant. An increase in the number of stereo-specifically bound cross-bridges leads to a significant reduction in $I_{1,0}$ while the increase in $I_{1,1}$ is small. Squares and circles are normalized experimental values for $I_{1,1}$ and $I_{1,0}$, respectively, before and after the first and second T-jumps (Fig. 4). The fraction of the cross-bridges bound to actin stereo-specifically at each temperature was estimated from the intensities of the A1 component in the first layer line (Fig. 11, Table 1) assuming that this fraction is proportional to the square root of the A1 intensity (see Discussion and Fig. 16).

I_{M3} intensity

The meridional reflection on M3 is the only bright Bragg x-ray reflection from actively contracting muscle apart from the equatorial reflections. It arises from the ~14.5-nm axial repeat of the layers of myosin cross-bridges on the three-stranded helix of the myosin filament. I_{M3} depends on several factors, such as the orientation of the cross-bridges with respect to the fiber axis, the number of cross-bridges attached to actin, the deviation of their axial positions from

the 14.5-nm repeat, and axial disorder of neighboring myosin filaments. When contracting intact muscle (Huxley et al., 1981, 1983) or muscle fibers (Irving et al., 1992; Lombardi et al., 1995; Piazzesi et al., 1995) are suddenly shortened or stretched, I_{M3} decreases temporarily. The time course of the decrease in I_{M3} is approximately simultaneous with the fast partial tension recovery following the length step and occurs in milliseconds (Irving et al., 1992; Lombardi et al., 1995). Because the mechanical and structural changes induced by a length step are reversed by returning the muscle length to its initial level 1–4 ms after the first step (Huxley et al., 1983; Lombardi et al., 1995), the population of myosin cross-bridges attached to actin does not change when I_{M3} decreases following the step. Because the number of diffractors and of myosin cross-bridges attached to the thin filaments remains constant for 1–2 ms after the length step, the decrease in I_{M3} following a length step most probably results from a tilting of a substantial part of the cross-bridges to a position more aligned along the fiber axis (Huxley at al., 1983; Irving et al., 1992). In permeabilized and slightly cross-linked muscle fibers, I_{M3} also decreases following releases and stretches (Bershitsky et al., 1996) at both low and high temperature (Bershitsky et al., 1997). In contrast to the length steps, an increase in temperature to ~17 and ~30°C led to an increase in I_{M3} by 20 and 41% (Fig. 6), which, however, was not instantaneous, but rather followed the slow component of the tension rise. This slow component was shown to be accompanied by a reattachment of the cross-bridges because, during this phase of the T-jump-induced tension transients, the cross-bridges forget the length changes applied before the T-jump in muscle fibers of the frog (Tsaturyan and Bershitsky, 1988) and rabbit (Bershitsky and Tsaturyan, 1992).

In an earlier paper (Bershitsky et al., 1997), only a small increase (6 ± 10%, mean ± SD, $n = 13$) in I_{M3} was observed following the T-jump from 5–6°C to ~20°C when I_{M3} values were compared at the plateau of contraction at these two temperatures. In the protocol used in the early paper, step releases and stretches were applied before the T-jump, and I_{M3} did not recover completely after the length perturbations, but remained 7% lower at the time of the T-jump application (Fig. 2 in Bershitsky et al., 1997). For this reason, I_{M3} at the plateau of contraction at ~20°C normalized for that just before the T-jump was (113 ± 11)% (mean ± SD). In the set of experiments presented here, the increase in I_{M3} was more pronounced (120 and 140% at ~17 and ~30°C, respectively). The most probable reason for the difference is the variation in I_{M3} from fiber to fiber.

In rigor, I_{M3} decreases when temperature rises, and the decrease correlates with the decrease in tension caused by thermal expansion of the contractile proteins (Bershitsky and Tsaturyan, 1985, 1989; Goldman et al., 1987; Davis and Harrington, 1987). This observation complements the increase in I_{M3} that accompanies the increase in tension induced by stretch of muscle fibers in rigor (Poole and Rapp. 1991; Bershitsky et al., 1996; Dobbie et al., 1997, 1998). Generally, in both rigor and active isometric contraction, I_{M3} changes in parallel with tension when temperature increases, whereas tension increases with temperature during contraction and decreases in rigor (Figs. 8 and 14).

Actin layer lines

The intensity of A1 during active contraction was, in our experiments, somewhat higher and the intensity of M1 was lower than those found in intact muscle (Huxley et al., 1982; Amemiya et al., 1987; Yagi, 1991; Bordas et al., 1991). The difference in the A1 intensity most probably results from the contribution of cross-linked myosin cross-bridges to A1 in our experiments. The cross-linking was performed when fibers were in rigor and when all myosin cross-bridges were strongly bound to actin. Stiffness measurements indicate that the percentage of cross-linked myosin cross-bridges in our conditions is 10–20% (Bershitsky et al., 1996). The A1 intensity in contracting muscle measured by Yagi (1991), who used the same range of radial integration, was 7.6% of the M1 intensity at rest. The x-ray intensity of A1 is approximately proportional to the square of the number of myosin heads labeling the actin helix (Huxley et al., 1982; Huxley and Kress, 1985). For any actin filament where helical order is well preserved, the myosin heads stereospecifically attached to the filament are coherent diffractors, and the square root of the normalized contribution of A1 in the first layer line in contracting muscle, n_A, is roughly proportional to the fraction of myosin heads having actin-based helical order. Therefore, the 7.6% intensity measured by Yagi (1991) corresponds to $n_A = 27.5\%$ ($\sqrt{0.076}$) in whole frog muscle at 5°C. The n_A value estimated from our data at the same temperature gives a figure of 34.8% ($\sqrt{0.121}$), which is 7.3% higher. The difference is less than the number of the cross-linked myosin heads estimated from stiffness measurement in the super-relaxing solution (Figs. 5 and 6) and can be explained by the contribution of the cross-linked heads to the A1 intensity because some of them might be cross-linked in a state stereo-specifically bound to actin.

The difference in the M1 intensity during active contraction in our experiment (4.6% at 5°C) and that measured in whole muscle in the same conditions (23–30%, Huxley et al., 1982; Yagi, 1991) is, however, too big to be explained by the effect of slight EDC cross-linking. To account for the difference between our results and those obtained on whole muscle, we consider factors that may decrease the intensity of M1 from the value of 23–30% in whole muscle to 4.6% in permeabilized, slightly cross-linked fibers. A difference of 15–20% may arise if such a fraction of fibers remained at rest during contraction of whole muscle, perhaps as a consequence of activation failure brought about by radiation damage. In this case, the estimation of the A1 component obtained from these specimens should be multiplied by a factor of 1.18–1.25 (= 1/0.85–1/0.8), so that the value of 7.6% estimated by Yagi (1991) increases to 8.9–9.5%, which is even closer to the 12.1% estimated from our data at 5–6°C.

We described previously the increase in the intensity of the hybrid A1/M1 layer line with temperature and measured the spacing of the differential peak, which was close to the position of A1 (Bershitsky et al., 1997). This result suggests that an increase in force with temperature is accompanied by more intense labeling of the actin helix by myosin cross-bridges. In the series of experiments described here, less noise and higher final temperature and tension were achieved than previously. Also, relaxed and rigor diffraction patterns were recorded for the same fibers. Thus, the A1 and M1 components of the reflections could be extracted from the active diffraction patterns at each temperature.

The relative contribution of A1 and M1 in the layer line could be estimated by taking advantage of the difference in their spacing (Fig. 10). When isometric force increases with temperature, the off-meridional x-ray intensity of the A1/M1 shifts along the meridian toward the position of A1, so that its contribution increases while the contribution of M1 decreases (Figs. 10 and 11 and Table 1). In contracting fibers, the sum of A1 and M1 contributions increased from 16.7% of its value in rigor to 37.8% at ~30°C showing that the cross-bridges become more ordered when they generate more force at the higher temperature. This increase in order is also seen in the decrease in the background level around the first layer line (Fig. 10).

When force increases by 1.84 times with temperature, n_A increases 1.71 times from 34.8 to 59.6% (Fig. 16). The fact that the estimated number of stereo-specifically bound heads is nearly proportional to force while stiffness and the total number of heads interacting with actin remain constant indicates that force is produced by a transition of nonstereo-specifically attached cross-bridges to the stereo-specific binding state.

Radial distribution of the intensity along A1 in contracting muscle was similar to that in rigor (Fig. 12). The only difference was a small off-meridional shift. This shift may result from a difference in conformation of myosin cross-bridges stereo-specifically bound to actin in contracting muscle from that in rigor. Alternatively, the α-helical necks of myosin S1 can be more disordered in contracting muscle where they bear a substantial force so that their contribution to the inner part of the layer line is reduced compared to rigor.

Further evidence for a transition of myosin cross-bridges to a state where they are stereo-specifically bound to actin is the shift of the intensity of A6 at ~$(5.9\ \text{nm})^{-1}$ toward the meridian (Fig. 10). Such a shift was found in rigor (Huxley and Brown, 1967), but not during active contraction at low temperature (Wakabayashi and Amemiya, 1991) whereas the A6 intensity, I_{A6}, increases when intact muscle develops isometric tension (Wakabayashi et al., 1985; Kress et al., 1986; Wakabayashi and Amemiya. 1991). An increase in I_{A6} during contraction is partially due to an activation of the thin filaments, but mainly results from attachment of myosin cross-bridges (Kress et al., 1986). The absence of a shift of the peak toward the meridian during contraction indicates that the majority of the cross-bridges attached to actin are not bound stereo-specifically, in contrast to rigor, because their neck regions, located at a higher radius from the axis of the thin filament (and therefore at a smaller reciprocal radius), do not contribute much to the inner part of A6. The response to an increase in temperature, which results in increased force, is quite different: after the T-jump, the peak of the intensity in A6 moves slightly toward the meridian, indicating that more myosin cross-bridges label the actin helix even at higher radii from the filament axis.

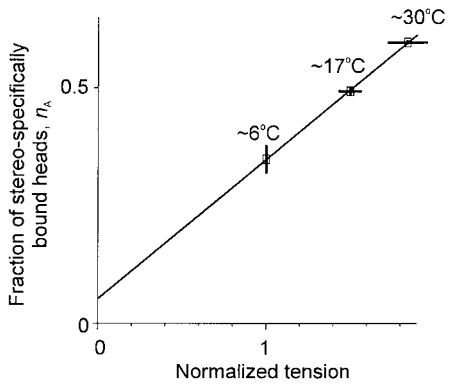

FIGURE 16 Plot of the fractions, n_A, of myosin cross-bridges contributing to A1 at different temperature against tension normalized for its value at 5–6°C. The fractions of the total number of myosin cross-bridges attached to the thin filaments in rigor were calculated as the square roots of the normalized A1 intensity (Table 1). The line is the linear regression through the data points, the error bars are SE. obtained from fiber-to-fiber statistics (for tension) and peak from the XFIT program (for the amplitude of the A1).

Possible implication for the mechanism of force generation

The data presented here support the view that muscle force generated upon raising temperature results from a transition of the cross-bridges from nonstereo-specific attachment to actin to a stereo-specific binding (Huxley and Kress, 1985; Harford and Squire, 1992; Brenner and Yu, 1993), while the total number of cross-bridges interacting with actin does not change significantly. The number of myosin heads stereo-specifically bound to actin in frog muscle fibers during isometric contraction at 5–6°C was estimated from the intensity of A1 to be ~35% (Fig. 16). This value is probably overestimated due to a contribution of the myosin cross-linked myosin heads and, possibly, of nonstereo-specifically bound heads to the A1 intensity. An estimate of 30% is more realistic and agrees well with that derived from the A1 intensity in intact muscle at the same temperature (Yagi, 1991). EPR studies (Cooke et al., 1984; Ostap et al., 1995) report that only 20–30% of the cross-bridges are tightly bound to actin in contracting rabbit muscle fibers at 22°C. Electron microscopy study of quickly frozen rabbit muscle fibers (Hirose et al., 1993) and fluorescent polarization of labels attached to the light chains of the myosin heads (Ling

et al., 1996; Hopkins et al., 1998) also show only a small fraction of cross-bridges bound to actin in a stereo-specific manner in contracting muscle. In frog muscle at this temperature, we report a higher fraction of stereo-specifically bound attached cross-bridges. However, it may be more relevant to compare rabbit muscle at 20°C to frog muscle at 5–6°C, where both data sets report 20–30% tightly bound cross-bridges. Indeed, both frog muscle at 5–6°C and rabbit muscle at 20°C show an ~1.6-fold enhancement of force when temperature rises by ~15°C (Bershitsky et al., 1997, Ranatunga, 1990), whereas, when frog muscle temperature rises from 20 to 30°C, force only increases ~1.1-fold. When tension rises with temperature, the A1 intensity increases so that as much as 60% of the cross-bridges become stereo-specifically bound (Table 1). Again, taking into account the cross-linked cross-bridges, ~55% of noncross-linked cross-bridges label the actin helix when active force increases by a factor of 1.84.

The number of cross-bridges attached to actin in contracting frog muscle fibers was estimated from stiffness measurements by Goldman and Simmons (1977) and more recently by Linari et al. (1998), who took into account a nonlinear strain–stress diagram in rigor (Higuchi et al., 1995) and the compliance of the thin and thick filaments (Suzuki and Sugi, 1983; Huxley et al., 1994; Wakabayashi et al., 1994). These measurements give an estimate of 43% of the cross-bridges contributing to active stiffness, if a cross-bridge is as stiff in contracting muscle as in rigor. Measurement of the equatorial x-ray intensities (Haselgrove and Huxley, 1973; Huxley and Kress, 1985) provide higher estimate (up to 90%) of the number of cross-bridges interacting with actin. A similar figure of >70% of the cross-bridges forming complexes with actin was obtained from analysis of the intensities of a number of meridional x-ray reflections by Martin-Fernandez et al. (1994). The figure of 55% myosin heads labeling the actin helix indicates that a majority of cross-bridges attached to actin become stereo-specifically bound when force approaches the upper limit of its physiological range with temperature.

An alternative hypothesis assumes that force generation occurs as a result of a transition of attached cross-bridges between two or more discrete states (Huxley and Simmons, 1971). A modern version of this hypothesis may suggest that the catalytic domain of a myosin head does not change conformation during the force-generating step, and only the α-helical neck and the light chains are involved in a tilting movement that results in force production (Holmes, 1997). Even if the lowest estimate for the number of cross-bridges attached to actin is used (43%, Linari et al., 1998) and assuming that their catalytic domains are strongly bound, the intensity of A1 during active contraction at 5°C would be as high as 18% of that in rigor. This is about twice as much as that observed in intact muscle (Yagi, 1991) and is 1.5 times higher than that found here in partially cross-linked muscle fibers (Table 1). One can argue that a tilt in the neck region of the myosin heads could be responsible for a decrease in the A1 intensity. However model calculations show that random axial and azimuthal tilt of the neck with a standard deviation of 30° (~4.5 nm) could be responsible for only an ~10% decrease in the contribution of a myosin head to the A1 intensity (Koubassova and Tsaturyan, paper in preparation). So, during an isometric contraction with 43% of attached heads, one would expect as much as $0.43 \times 0.43 \times 0.9 = 16.6\%$ of the A1 intensity in rigor if their catalytic domains are stereo-specifically bound to actin and only the necks undergo a high amplitude tilting. Also, only 20% of spin-labels attached to the catalytic domain of S1 were found strongly bound to actin in contracting muscle (Cooke et al., 1984). Huxley et al. (1982) indicated that the cross-bridges attached to actin in contracting muscle are rather well ordered axially, but probably disordered azimuthally. It was pointed out by A. F. Huxley (personal communication) that an increase in the A1 intensity and a shift of the A6 peak toward the meridian that accompany the temperature-induced increase in force can be explained in terms of the Huxley–Simmons (1971) model as follows. In this model, isometric contraction is an equilibrium between a low-force and a high-force state of the attached cross-bridges, and a temperature jump would shift this equilibrium in favor of the high-force state. Both states must be stiff in the axial direction to explain the constancy of stiffness of the whole fiber, but, if cross-bridges in the low-force state (i.e., the state described as nonstereo-specific in the work presented here) were free to rotate about the fiber axis, their orientations would not follow the long helix of the thin filament and therefore they would not contribute to the actin layer lines. The slow increase in the intensity of the M3 meridional reflection with temperature observed here is more difficult to accommodate in this model.

The Huxley–Simmons model (1971) is supported by the measurements of the M3 meridional intensity following fast changes in length of whole muscles (Huxley et al., 1981; Husley et al., 1983) or single intact (Irving et al., 1992; Lombardi et al., 1995; Piazzesi et al., 1995) and permeabilized (Bershitsky et al., 1996, 1997) fibers. After either release or stretch, the M3 intensity decreases dramatically, whereas the brightness of the equatorial intensities and of the first layer line (Huxley et al., 1983) do not change noticeably. The decrease in the M3 intensity occurs not during the step itself, but accompanies the fast partial tension recovery after the step is complete (Irving et al., 1992). These data are evidence for a tilting of a significant part of the cross-bridges attached to actin because the changes in M3 are reversible within 1–2 ms after the step (Huxley et al., 1983) and no signs of radial movement are seen on the x-ray diffraction patterns. Small changes in axial orientation of fluorescent probes attached to the regulatory myosin light chains in response to the length steps were also found (Irving et al., 1995; Hopkins et al., 1998). If a force-generating transition is accompanied by tilting of a majority of the cross-bridges to a state where they are more aligned with the fiber axis, one would expect a substantial decrease in the M3 intensity with temperature when force increases

by 1.84. Instead, we observed a relatively slow increase in I_{M3} by 41% (Fig. 8), nearly a 3-fold increase in the intensity of I_{A1} and a 26% decrease in $I_{1,0}$. So the changes in the x-ray diffraction induced by the length steps are different from those observed when generation of higher force is stimulated by an increase in temperature at isometric conditions. The changes in I_{M3} suggest that force generation is more complex than the mechanism presented by Huxley and Simmons (1971).

Because isometric tension is proportional to the number of the cross-bridges labeling the actin helix (Fig. 16), we conclude that muscle force results from a transition of nonstereo-specifically attached myosin heads to a stereo-specifically bound state.

We are grateful to Professor Sir Andrew F. Huxley for his constructive comments on the draft paper, to Dr. David R. Trentham for his help with the manuscript and to the non-crystalline diffraction team of CCLRC Daresbury Laboratory for the hard- and software support, to Dr. M. Webb for supplying us with chicken phosphocreatine kinase, and Tagdem Ural Co., Yekaterinburg, for providing laboratory space for Dr. S. Bershitsky. The work was supported by grants from INTAS, RFBR, HHMI, and by MRC, CCP13 of EPSRC and BBSRC and by Daresbury Laboratory. R. Burns was an MRC Ph.D. student.

REFERENCES

Amemiya, Y., K. Wakabayashi, H. Tanaka, Y. Ueno, and J. Miyahara. 1987. Laser-stimulated luminescence used to measure x-ray diffraction of a contracting striated muscle. *Science*. 237:164–168.

Bershitsky, S. Y., and A. K. Tsaturyan. 1985. Effect of submillisecond temperature jump on tension in skinned skeletal muscle fibres of the frog in the rigor state. *Biofizika*. 30:868–871 (in Russian).

Bershitsky, S. Y., and A. K. Tsaturyan. 1986. Thermoelastic properties of the cross-bridges in permeabilised muscle fibres of the frog in rigor state. *Biofizika*. 31:532–533 (in Russian).

Bershitsky, S. Y., and A. K. Tsaturyan. 1988. Biphasic tension response to temperature jump in Ca^{2+} activated muscle fibres from the frog. *Biofizika*. 33:147–149 (in Russian).

Bershitsky, S. Y., and A. K. Tsaturyan. 1989. Effect of Joule temperature jump on tension and stiffness of permeabilised muscle fibers. *Biophys. J.* 56:809–816.

Bershitsky, S. Y., and A. K. Tsaturyan. 1992. Tension responses to Joule temperature jump in skinned rabbit muscle fibres. *J. Physiol.* 447: 425–448.

Bershitsky, S. Y., and A. K. Tsaturyan. 1995a. Force generation and work production by covalently cross-linked actin–myosin cross-bridges in rabbit muscle fibers. *Biophys. J.* 69:1011–1021.

Bershitsky, S. Y., and A. K. Tsaturyan. 1995b. Slight EDC cross-linking stabilises sarcomere structure and preserves mechanical properties of permeabilised frog muscle fibres. *J. Physiol*. 483:76P–77P.

Bershitsky, S. Y., A. K. Tsaturyan, O. N. Bershitskaya, G. I. Mashanov, P. Brown P., M. Webb, and M. A. Ferenczi. 1996. Mechanical and structural properties underlying contraction of skeletal muscle fibers after partial 1-ethyl-[3-(3-dimethylamino)propyl]carbodiimide cross-linking. *Biophys. J.* 71:1462–1474.

Bershitsky, S. Y., A. K. Tsaturyan, O. N. Bershitskaya, G. I. Mashanov, P. Brown, R. Burns, and M. A. Ferenczi. 1997. Muscle force is generated by myosin heads stereospecifically attached to actin. *Nature*. 388: 186–190.

Bershitsky, S. Y., A. K. Tsaturyan, R. Burns, and M. A. Ferenczi. 1998. Structural changes in permeabilised frog muscle fibres following flash photolysis of DMB-caged ATP and DMB-caged ADP. *J. Muscle Res. Cell Motil.* 19:281.

Bordas, J., G. P. Diakun, J. E. Harries, R. A. Lewis, M. L. Martin-Fernandez, and E. Towns-Andrews. 1991. Two-dimensional X-ray diffraction of muscle: recent results. *Adv. Biophys.* 27:15–33.

Bordas, J., G. Diakum, F. Dias, J. Harris, R. Lewis, J. G. Mant, M. Fernandez, and E. Towns-Andrews. 1993. Two dimensional time-resolved x-ray diffraction studies of live isometrically contracting frog sartorius muscle. *J. Muscle Res. Cell Motil.* 14:314–324.

Brenner, B., J. M. Chalovich, and L. C. Yu, 1995. Distinct molecular processes associated with isometric force generation and rapid tension recovery after quick release. *Biophys. J.* 68:106s–111s.

Brenner, B., and L. C. Yu, 1985. Equatorial x-ray diffraction from single skinned rabbit psoas fibres at various degrees of activation. Changes in intensities and lattice spacing. *Biophys. J.* 48:829–834.

Brenner, B., and L. C. Yu. 1993. Structural changes in the actomyosin cross-bridges associated with force generation. *Proc. Natl. Acad. Sci. USA.* 90:5252–5256.

Cooke, R., M. S. Crowder, C. H. Wendt, V. A. Barnett, and D. D. Thomas. 1984. Muscle cross-bridges: do they rotate? *In* Contractile Mechanisms in Muscle. Plenum Press, New York, London. 413–423.

Davis, J. S., and W. F. Harrington. 1987. Force generation by muscle fibers in rigor: a laser temperature-jump study. *Proc. Natl. Acad. Sci. USA.* 84:975–979.

Davis, J. S., and W. F. Harrington. 1993. A single order–disorder transition generates tension during the Huxley–Simmons phase 2 in muscle. *Biophys. J.* 65:1886–1898.

Davis, J. S., and M. E. Rodgers. 1995. Force generation and temperature-jump and length-jump tension transients in muscle fibers. *Biophys. J.* 68:2032–2040.

Dobbie, I., M. Irving, M. Reconditi, M. Linari, N. Koubasova, G. Piazzesi, and V. Lombardi. 1997. Tension dependent structural changes of actin–myosin cross-bridges in rigor. *Biophys. J.* 72:A277.

Dobbie, I., M. Linari, G. Piazzesi, M. Reconditi, N. Koubasova, M. A. Ferenczi, V. Lombardi, and M. Irving. 1998. Elastic bending and active tilting of myosin heads during muscle contraction. *Nature*. 396:383–387.

Ford, L. E., A. F. Huxley, and R. M. Simmons. 1977. Tension responces to sudden length change in stimulated frog muscle fibers near slack length. *J. Physiol.* 269:441–515.

Goldman, Y. E., J. A. McCray, and K. W. Ranatunga. 1987. Transient tension changes initiated by laser temperature jump in rabbit psoas muscle fibres. *J. Physiol.* 392:71–95.

Goldman, Y. E., and R. M. Simmons. Active and rigor muscle stiffness. 1977. *J. Physiol.* 269:55P–57P.

Harford, J. J., and J. M. Squire. 1992. Evidence for structurally different attached states of myosin cross-bridges on actin during contraction of fish muscle. *Biophys. J.* 63:387–396.

Haselgrove, J. C., and H. E. Huxley. 1973. X-ray evidence for radial cross-bridge movement and for the sliding filament model in actively contracting skeletal muscle. *J. Mol. Biol.* 77:549–568.

Higuchi, H., T. Yanagida, and Y. E. Goldman. 1995. Compliance of thin filaments in skinned fibers of rabbit skeletal muscle. *Biophys. J.* 69: 1000–1010.

Hill, A. V. 1931. Myothermic experiments on a frog gastrocnemius. *Proc. Roy. Soc. B.* 109:267–303.

Hirose, K., T. D. Lenart, J. M. Murray, C. Franzini-Armstrong, and Y. E. Goldman. 1993. Flash and smash: rapid freezing of muscle fibers activated by photolysis of caged ATP. *Biophys. J.* 65:397–408.

Holmes, K. C. 1997. The swinging lever-arm hypothesis of muscle contraction. *Current Biology*. 7:R112–R118.

Hopkins, S. C., C. Sabido-David, J. E. T. Corrie, M. Irving, and Y. E. Goldman. 1998. Fluorescence polarization transient from rhodamine isomers on the myosin regulatory light chain in skeletal muscle fibers. *Biophys. J.* 74:3093–3110.

Huxley, A. F. 1981. The mechanical properties of cross-bridges and their relation to muscle contraction. *In* Advances in Physiological Sciences, Vol. 5. E. Varga, A. Kövér, T. Kovács, L. Kovács, editors. Pergamon Press and Akadémiai Kiadó, Budapest. 1–12.

Huxley, A. F., and R. M. Simmons. 1971. Proposed mechanism of force generation in striated muscle. *Nature*. 233:533–538.

Huxley, H. E. 1969. The mechanism of muscular contraction. *Science*. 164:1356–1366.

Huxley, H. E., and W. Brown. 1967. The low-angle X-ray diagram of vertebrate striated muscle and its behaviour during contraction and rigor. *J. Mol. Biol.* 30:383–434.

Huxley, H. E., A. R. Faruqi, M. Kress, J. Bordas, and M. H. J. Koch. 1982. Time resolved X-ray diffraction studies of the myosin layer line reflections during muscle contraction. *J. Mol. Biol.* 158:637–684.

Huxley, H. E., and M. Kress. 1985. Crossbridge behaviour during muscle contraction. *J. Musc. Res. Cell Motil.* 6:153–161.

Huxley, H. E., R. M. Simmons, A. R. Faruqi, M. Kress, J. Bordas, and M. H. Koch. 1981. Millisecond time-resolved changes in x-ray reflections from contracting muscle during rapid mechanical transients, recorded using synchrotron radiation. *Proc. Natl. Acad. Sci. USA.* 78: 2297–2301.

Huxley, H. E., R. M. Simmons, A. R. Faruqi, M. Kress, J. Bordas, and M. H. J. Koch. 1983. Changes in the X-ray reflections from contracting muscle during rapid mechanical transients and their structural implications. *J. Mol. Biol.* 169:469–506.

Huxley, H. E., A. Stewart, H. Sosa, and T. Irving. 1994. X-ray diffraction measurement of the extensibility of actin and myosin in contracting muscle. *Biophys. J.* 67:2411–2421.

Irving, M., T. St. C. Allen, C. Sabido-David, J. S. Craik, B. Brandmeier, J. Kendrick-Jones, J. E. T. Corrie, D. R. Trentham, and Y. E. Goldman. 1995. Tilting of the light-chain region of myosin during step length changes and active force generation in skeletal muscle. *Nature*. 375: 688–691.

Irving, M., V. Lombardi, G. Piazzesi, and M. A. Ferenczi. 1992. Myosin head movements are synchronous with the elementary force-generating process in muscle. *Nature*. 357:156–158.

Kress, M., Huxley, H. E., Faruqi, A. R., and J. Hendrix. 1986. Structural changes during activation of frog muscle studied by time-resolved X-ray diffraction. *J. Mol. Biol.* 188:325–342.

Linari, M., I. Dobbie, M. Reconditi, N. Koubassova, M. Irving, G. Piazzesi, and V. Lombardi. 1998. The stiffness of skeletal muscle in isometric contraction and rigor: the fraction of myosin heads bound to actin. *Biophys. J.* 74:2459–2473

Ling, N., C. Shrimpton, J. Sleep, J. Kendrick-Jones, and M. Irving. 1996. Fluorescent probes of orientation of myosin regulatory light chains in relaxed, rigor and contracting muscle. *Biophys. J.* 70:1836–1846.

Lombardi, V., G. Piazzesi, M. A. Ferenczi, H. Thirlwell, and M. Irving, M. 1995. Elastic distortion of myosin heads and repriming of the working stroke in muscle. *Nature*. 374:553–555.

Lovell, S. J., P. J. Knight, and W. F. Harrington. 1981. Fraction of myosin heads bound to thin filaments in rigor fibrils from insect flight and vertebrate muscles. *Nature*. 293:664–666.

Malinchik, S., and L. C. Yu. 1995. Analysis of equatorial x-ray diffraction patterns from muscle fibers: factors that affect the intensities. *Biophys. J.* 68:2023–2031.

Martin-Fernandez, M. A., J. Bordas, G. Diakun, J. Harris, J. Lowy, G. R. Mant, A. Svensson, and E. Towns-Andrews. 1994. Time-resolved X-ray diffraction studies of myosin head movements in live frog sartorius muscle during isometric and isotonic contractions. *J. Musc. Res. Cell Motil.* 15:319–348.

Ostap, E. M., V. A. Barnett, and D. D. Thomas. 1995. Resolution of three structural states of spin-labeled myosin in contracting muscle. *Biophys. J.* 69:177–188.

Piazzesi, G., V. Lombardi, M. A. Ferenczi, H. Thirlwell, I. Dobbie, and M. Irving. 1995. Changes in the x-ray diffraction pattern from single, intact muscle fibers produced by rapid shortening and stretch. *Biophys. J.* 68:92s–98s.

Poole, K. J. V., and G. Rapp. 1991. X-ray diffraction measurements on the effect of rapid length changes in rigor cross-bridges in skinned rabbit psoas fibres. *Biophys. J.* 59:575a.

Ranatunga, K. W. 1990. Temperature sensitivity of isometric tension in glycerinated mammalian muscle fibres. *In* Muscle and Motility. G. Marechal and U. Carraro, editors. Intercept Ltd., Andover, U.K. 271–276.

Ranatunga, K. W. 1996. Endothermic force generation in fast and slow mammalian (rabbit) muscle fibers. *Biophys. J.* 71:1905–1913.

Rapp, G. J., and J. S. Davis. 1996. X-ray diffraction studies on thermally induced tension generation in rigor muscle. *J. Muscle Res. Cell Motil.* 17:617–629.

Rayment, I., H. M. Holden, M. Whittaker, C. B. Yohn, M. Lorenz, K. Holmes, and R. Milligan. 1993. Structure of the actin–myosin complex and its implication for muscle contraction. *Science*. 261:58–65.

Reedy, M. K., K. C. Holmes, and R. T. Tregear. 1965. Induced changes in the orientation of the cross-bridges of glycerinated insect fight muscle. *Nature*. 207:1276–1280.

Suzuki S., and H. Sugi. 1983. Extensibility of the myofilaments in vertebrate skeletal muscle as revealed by stretching rigor muscle fibers. *J. Gen. Physiol.* 81:531–546.

Towns-Andrews E., A. Berry, J. Bordas, G. R. Mant, P. K. Murray, K. Roberts, I. Sumner, J. S. Worgan, and R. Lewis. 1989. Time-resolved x-ray diffraction station: x-ray optics, detectors and data acquisition. *Rev. Scient. Instrument.* 60:2346–2349.

Tsaturyan, A. K., and S. Y. Bershitsky. 1988. Tension responses to the temperature jump on skinned Ca^{2+}-activated muscle fibers of the frog after the stepwise length change. *Biofizika*. 33:570–572. (in Russian)

Wakabayashi, K., and Y. Amemiya. 1991. Progress in x-ray synchrotron diffraction studies of muscle contraction. *In* Handbook on Synchrotron Radiation. 4:597–678.

Wakabayashi, K., H. Tanaka, Y. Amemiya, A. Fujishima, T. Kobayashi, T. Hamanaka, H. Sugi, and T. Mitsui. 1985. Time resolved X-ray diffraction studies on the intensity changes of the 5.9 and 5.1 nm actin layer lines from frog skeletal muscle during an isometric tetanus using synchrotron radiation. *Biophys. J.* 47:847–850.

Wakabayashi, K., Y. Sugimoto, H. Tanaka, Y. Ueno, Y. Takezawa, and Y. Amemiya. 1994. X-ray diffraction evidence for the extensibility of actin and myosin filaments during muscle contraction. *Biophys. J.* 67: 2422–2435.

Worgan, J. S., R. A. Lewis, N. S. Fore, I. L. Sumner, A. Berry, A. Parker, F. D'Annunzio, M. L. Martin-Fernandez, E. Towns-Andrews, J. E. Harris, G. R. Mant, G. P. Diakun, and J. Bordas. 1990. The application of multiwire X-ray detectors to experiments using synchrotron radiation. *Nucl. Inst. Method Phys. Res.* A291:447–454.

Yagi, N. 1991. Intensification of the first actin layer-line during contraction of frog skeletal muscle. *Adv. Biophys.* 27:35–43.

Yu, L. C., J. E. Hartt, and R. J. Podolsky. 1979. Equatorial x-ray intensities and isometric force levels in frog sartorius muscle. *J. Mol. Biol.* 132: 53–67.